On Intermediate Models for Barotropic Continental Shelf and Slope Flow Fields. Part I: Formulation and Comparison of Exact Solutions

J. S. ALLEN, J. A. BARTH AND P. A. NEWBERGER

College of Oceanography, Oregon State University, Oceanography Admin Bldg 104, Corvallis, OR 97331-5503

(Manuscript received 17 May 1989, in final form 18 December 1989)

ABSTRACT

Motivated by the general objective of pursuing oceanographic process and data assimilation studies of the complex, nonlinear eddy and jet current fields observed over the continental shelf and slope off the west coast of the United States, we investigate the use of intermediate models for that purpose. Intermediate models contain physics between that in the primitive equations and that in the quasigeostrophic equations and are capable of representing subinertial frequency motion over the O(1) topographic variations typical of the continental slope, while filtering out high-frequency gravity-inertial waves. As an initial step, we compare and evaluate several intermediate models applied to the *f*-plane shallow-water equations for flows over topography. The accuracy and utility of the intermediate models are assessed by a comparison of exact analytical and numerical solutions with those of the primitive shallow-water equations (SWE) and with those of the quasi-geostrophic equations (QG). The intermediate models that we consider are based on the geostrophic momentum (GM) approximation, the derivation of Salmon (1983) utilizing Hamilton's principle (HP), a geostrophic vorticity (GV) approximation, the quasi-geostrophic momentum and full continuity equations (IM), the linear balance equations (LBE), the balance equations (BE), the related balance-type (HBE, BEM, NBE) and modified linear balance equations (LQBE), the slow equations (SE) of Lynch (1989), and the modified slow equations (MSE). In Part I, we discuss the intermediate models and develop formulations that are suitable for numerical solution in physical coordinates for use in Parts II and III. We investigate the capability of the intermediate models to represent linear ageostrophic coastally trapped waves, i.e., Kelvin and continental shelf waves, and demonstrate that they do so with accuracy consistent with standard linear low-frequency approximations. We also assess the accuracy of the models by a comparison of exact nonlinear analytical solutions to the SWE for steady flow in an elliptic paraboloid and for unsteady motion of elliptical vortices in a circular paraboloid with corresponding analytical solutions to the intermediate models and to QG. General results from the exact solution comparisons include the following. Many of the intermediate models are capable of producing more accurate solutions than QG over a range of Rossby numbers $0 < \epsilon < 1$. In some cases, the intermediate models provide accurate approximate solutions where QG is not applicable and fails to give a relevant solution. Considerable parameter-dependent variation in quality exists, however, among the different intermediate models. For the particular problems considered here, BE, HBE, BEM, NBE, and MSE reproduce the exact results of the SWE while LBE and LQBE give the same approximation as QG. The accuracy of the models is typically in the order GV, GM, IM, HP, and QG, with GV most accurate and IM and HP sometimes less accurate than QG.

1. Introduction

We are interested in understanding the dynamical processes involved in the formation and maintenance of the complicated eddy and jet current fields observed over the continental margin off the west coast of the United States (e.g., Kosro and Huyer 1986; Huyer and Kosro 1987). Since these flow fields appear to be strongly nonlinear, the use of an appropriate numerical model for process and data assimilation studies is indicated. Based on the success of a quasi-geostrophic model in data assimilation studies of mesoscale eddies in a nearby region offshore in the California Current (Robinson et al. 1984; Robinson et al. 1986) and on the assumption that the eddies and jets observed nearer to shore over the continental shelf and slope have reasonably similar time and space scales, we have been motivated to look for a model with the dynamical simplicity and robustness of quasi-geostrophy that will, in addition, remain valid over the O(1) topographic variations typical of the continental slope. Intermediate models (McWilliams and Gent 1980) seem to offer promising possibilities in this regard. These models contain physics intermediate between that in the quasi-geostrophic approximation and that in the full primitive equations. In particular, they are capable of representing flows over O(1) topographic variations, with accompanying O(1) variations in the height of density surfaces, for which the quasi-geostrophic approximation is not valid. In addition, intermediate models systematically filter out the high-frequency gravity–inertial waves present in the primitive equations. This latter

Corresponding author address: Dr. John S. Allen, College of Oceanography, Oregon State University, Oceanography Admin Bldg 104, Corvallis, OR 97331-5503.

fact may lead to simplifications, relative to the primitive equations, in the application of intermediate models to data assimilation studies. In fact, although existing intermediate models have been developed with other atmospheric and oceanic flow problems in mind, the study of the mesoscale dynamics of oceanographic flow over the continental margin would seem to provide an obvious area for their application.

Intermediate model approximations were reviewed by McWilliams and Gent (1980). Since that time, these authors have completed a substantial amount of further study on intermediate models in general (Gent and McWilliams 1982) and on the balance equations (BE) in particular (Gent and McWilliams 1983a,b; Gent and McWilliams 1984; Norton et al. 1986; McWilliams et al. 1986). The geostrophic momentum (GM) approximation described by Hoskins (1975) results in another intermediate model that has been widely used in the study of atmospheric motions (e.g., Hoskins 1982). The GM approximation is frequently employed in conjunction with a transformation to geostrophic coordinates, after which the model is referred to as the semigeostrophic equations.

Although different intermediate models have been derived and have existed for several years, there remains in general a shortage of numerical solutions, comparative studies, and model evaluations. We note that our objective of employing the model for data assimilation studies in fixed geographical locations, essentially requires that solutions be obtained in physical coordinates. For some intermediate models methods for obtaining numerical solutions in physical coordinates have not been formulated and for others the development of new procedures has been required (Norton et al. 1986). In particular, at present there exist no applications of intermediate models to oceanographic flow fields over bottom topography typical of the continental margin. As a consequence, our initial objective has been to understand the capabilities and limitations of different intermediate models and to assess the accuracy of their solutions for rotating, stratified oceanographic flows over topography.

In order to initiate a comparative study that begins to meet these objectives, we have chosen to apply a set of intermediate models to the *f*-plane shallow-water equations. Although in that case the effects of stratification are only partially represented by the free surface deformations, we felt that this would provide a valuable test in the simplest possible circumstance that would retain a great deal of the important physics. We note that the response to atmospheric forcing of currents on the continental shelf off the U.S. west coast is strongly influenced by dynamics associated with ageostrophic coastally trapped wave motions that have a strong barotropic component (e.g., Allen and Kundu 1978; Denbo and Allen 1987). These waves must be represented properly by any data assimilation model and it is clearly of benefit to investigate this matter first in the simplified context of the barotropic shallow-water equations.

We have proceeded with this comparative study by evaluating the accuracy of solutions from different intermediate models and from the quasigeostrophic approximation, relative to those from the primitive equations, for flows over topography. An extensive set of numerical finite-difference solutions for initial-value problems has been obtained and the results will be presented in Parts II (Barth et al. 1990) and III (Allen et al. 1990). We also assess the accuracy of the different intermediate models by comparing some exact nonlinear analytical solutions that exist for the shallow-water equations (Ball 1965; Cushman-Roisin et al. 1985), both with and without topography, with corresponding analytical solutions of the intermediate models. The exact solutions to the shallow-water equations hold for restricted circumstances and thus are not as general as those obtainable by numerical solution, but appear in this case to provide useful comparisons. Moreover, the opportunity to obtain analytical expressions for the errors introduced by various approximations in nonlinear solutions is rare and we feel that it should be exploited.

The outline of this paper is as follows. In section 2, we recall the shallow-water equations (SWE) and the resulting relations for potential vorticity and energy conservation. For comparison with the intermediate models, we also record the quasi-geostrophic (QG) approximation to these equations. In section 3, we present a number of intermediate models for the shallow-water equations. These include the geostrophic momentum (GM) approximation of Hoskins (1975), the geostrophic vorticity (GV) approximation (Sutyrin and Yushina 1986a,b), the equations (HP) of Salmon (1983) for nearly geostrophic flow, a model (IM) based on the quasi-geostrophic momentum and full continuity equations (Williams 1985; Cushman-Roisin 1986), the balance (BE) and linear balance equations (LBE) (e.g., Gent and McWilliams 1983a), and the slow equations (SE) of Lynch (1989). We also formulate and present a set of different balance-type equations (HBE, BEM, NBE), modified linear balance equations (LQBE), modified slow equations (MSE), and we further develop a geostrophic vorticity (GV) model. In several cases, we reduce the original model equations to a form that is appropriate for numerical solution in physical coordinates for use in Parts II and III. In section 4, we examine the behavior of the intermediate models in a limit for which we expect them to reduce to the quasi-geostrophic approximation and we evaluate the capability of the intermediate models to represent linear ageostrophic coastally trapped waves, i.e., Kelvin and continental shelf waves. In sections 5 and 6, we present exact solutions to the shallow-water equations and to the different intermediate models for steady flow in an elliptic paraboloid (Ball 1965) and for unsteady flow in a circular paraboloid. The latter time-dependent motions reduce to the Ro-

don solutions of Cushman-Roisin et al. (1985) in the absence of topography. A comparison of the exact solutions and a summary of results are given in sections 7 and 8. A summary of the equations for all of the intermediate models (except SE) and for QG, expressed in a common formulation related to that utilized for BE, is given in appendix C.

2. Formulation

a. *Shallow-water equations—SWE*

We concentrate on rotating fluid flows governed by the inviscid shallow-water equations (SWE) on an f-plane. Dimensionless variables similar to those in Pedlosky (1987) are utilized so that in Cartesian coordinates (x, y) the continuity and momentum equations are

$$\epsilon F\eta_t + (hu)_x + (hv)_y = 0, \tag{2.1a}$$

$$\epsilon u_t + \epsilon(uu_x + vu_y) - v = -\eta_x, \tag{2.1b}$$

$$\epsilon v_t + \epsilon(uv_x + vv_y) + u = -\eta_y, \tag{2.1c}$$

where

$$h = \epsilon F\eta + 1 - h_B, \tag{2.1d}$$

$\epsilon F\eta$ is the elevation of the free surface relative to the undisturbed depth of the fluid $H = 1 - h_B$ where $h_B(x, y)$ is the height of the bottom topography, (u, v) are velocity components in the (x, y) directions, and t is time. Subscripts (x, y, t) denote partial differentiation. There are two dimensionless parameters, the Rossby number ϵ and F,

$$\epsilon = U/(fL), \quad F = f^2L^2/(g\mathcal{D}), \tag{2.2a,b}$$

where L, $\mathcal{D}$, and U are characteristic values for, respectively, a horizontal scale, the undisturbed fluid depth, and a horizontal fluid velocity, f is the Coriolis parameter, and g is the acceleration of gravity. The parameter F is the square of the ratio of the horizontal length scale L to the Rossby radius of deformation $\delta_R = (g\mathcal{D})^{1/2}/f$. As in Pedlosky (1987), the dimensionless variables (x, y), t, (u, v), h_B, and η have been formed from their dimensional counterparts by using the characteristic scales L, L/U, U, $\mathcal{D}$, and $\epsilon F\mathcal{D}$, respectively.

We will find it convenient in many instances to utilize (2.1a, b, c) in the equivalent forms

$$\epsilon F\eta_t + (\hat{H}u)_x + (\hat{H}v)_y + D = 0, \tag{2.3a}$$

$$\epsilon u_t - (1 + \epsilon\zeta)v = -\mathcal{B}_x, \tag{2.3b}$$

$$\epsilon v_t + (1 + \epsilon\zeta)u = -\mathcal{B}_y, \tag{2.3c}$$

where

$$\mathcal{B} = \eta + \epsilon K, \quad K = \tfrac{1}{2}(u^2 + v^2), \tag{2.3d,e}$$

$$\hat{H} = \epsilon F\eta - h_B, \tag{2.3f}$$

$\mathcal{B}$ is the Bernoulli function,

$$\zeta = v_x - u_y, \tag{2.3g}$$

is the vertical component of relative vorticity, and

$$D = u_x + v_y, \tag{2.3h}$$

is the horizontal divergence.

An equation for ζ, readily derived from (2.3b, c), is

$$\epsilon(\zeta_t + u\zeta_x + v\zeta_y) + (\epsilon\zeta + 1)D = 0. \tag{2.4}$$

Likewise an equation for D,

$$\epsilon[D_t + uD_x + vD_y + D^2 + 2(v_xu_y - v_yu_x)] - \zeta = -\nabla^2\eta, \tag{2.5}$$

where ∇^2 is the horizontal Laplacian operator, also follows from (2.3b, c).

By combining (2.4) and (2.1a), we obtain

$$Q_t + uQ_x + vQ_y = 0, \tag{2.6}$$

where

$$Q = (1 + \epsilon\zeta)/h \tag{2.7}$$

is the potential vorticity which is thus conserved following fluid particles moving with velocity (u, v). The combination of (2.6) multiplied by hQ and (2.1a) multiplied by Q^2 yields an equation for the conservation of potential enstrophy density hQ^2,

$$(hQ^2)_t + (uhQ^2)_x + (vhQ^2)_y = 0. \tag{2.8}$$

A similar relation may be derived for an arbitrary function $Fn(Q)$ which replaces Q^2 in (2.8).

An additional useful equation

$$Q_{Lt} + (uQ_L)_x + (vQ_L)_y = 0, \tag{2.9a}$$

for

$$Q_L = \zeta - \tilde{H}, \tag{2.9b}$$

where

$$\tilde{H} = \hat{H}/\epsilon = F\eta - \epsilon^{-1}h_B, \tag{2.10}$$

follows from the subtraction of (2.3a) from (2.4).

The SWE (2.1) also imply the following relation expressing the conservation of energy,

$$\epsilon\left(hK + \frac{1}{2}F\eta^2\right)_t + (uh\mathcal{B})_x + (vh\mathcal{B})_y = 0. \tag{2.11}$$

Initial-boundary-value problems for (2.1) require the specification at $t = 0$ of $u(x, y, 0)$, $v(x, y, 0)$, and $\eta(x, y, 0)$ and the vanishing of the normal component of velocity at rigid boundaries.

b. *Quasi-geostrophic equations—QG*

We are interested in approximate solutions to the SWE (2.1) in the limiting case of small Rossby number, i.e., for

$$\epsilon \ll 1, \tag{2.12}$$

with, in general, $F = O(1)$. The standard approximation in this case results in a governing equation for quasi-geostrophic (QG) flow that is systematically derived in Pedlosky (1987) by expanding the variables in an asymptotic expansion in powers of ϵ. For comparison with the intermediate models, it is useful to recall the steps and the results of that derivation below.

The velocity components and interface height are expanded, e.g., as

$$\eta = \eta_0 + \epsilon\eta_1 + O(\epsilon^2), \tag{2.13}$$

where

$$u_0 = -\eta_{0y}, \quad v_0 = \eta_{0x}, \tag{2.14a,b}$$

$$\zeta_0 = v_{0x} - u_{0y} = \nabla^2\eta_0. \tag{2.15}$$

The $O(\epsilon)$ momentum equations are

$$u_{0t} - \zeta_0 v_0 - v_1 = -\mathcal{B}_{1x}, \tag{2.16a}$$

$$v_{0t} + \zeta_0 u_0 + u_1 = -\mathcal{B}_{1y}, \tag{2.16b}$$

where

$$\mathcal{B}_1 = \eta_1 + K_0, \quad K_0 = \frac{1}{2}(u_0^2 + v_0^2). \tag{2.16c,d}$$

The vorticity equation follows from (2.16):

$$\zeta_{0t} + u_0\zeta_{0x} + v_0\zeta_{0y} + D_1 = 0, \tag{2.17}$$

where

$$D_1 = u_{1x} + v_{1y}. \tag{2.18}$$

The continuity equation (2.1a) is approximated by

$$F\eta_{0t} - u_0\hat{h}_{Bx} - v_0\hat{h}_{By} + D_1 = 0, \tag{2.19}$$

where it is assumed that

$$\eta_0 = O(1), \quad \hat{h}_B = \epsilon^{-1}h_B = O(1). \tag{2.20a,b}$$

An equation for quasi-geostrophic potential vorticity,

$$Q_0 = \zeta_0 - F\eta_0 + \epsilon^{-1}h_B, \tag{2.21}$$

may be derived by eliminating D_1 from (2.17) and (2.19):

$$Q_{0t} + u_0Q_{0x} + v_0Q_{0y} = 0, \tag{2.22}$$

and it expresses the conservation of Q_0 following fluid particles moving with velocities (u_0, v_0). Eq. (2.22) may be written in terms of the single variable η_0,

$$(\nabla^2\eta_0 - F\eta_0)_t = -J(\eta_0, \nabla^2\eta_0 + \epsilon^{-1}h_B), \tag{2.23}$$

where the operator $J(a, b) = a_xb_y - b_xa_y$ is the Jacobian, and thus provides a single governing equation for quasi-geostrophic flow.

An equation for the conservation of QG potential enstrophy follows from the multiplication of (2.22) by Q_0:

$$Q_{0t}^2 + (u_0Q_0^2)_x + (v_0Q_0^2)_y = 0. \tag{2.24}$$

The QG approximation also implies a corresponding form of energy conservation which may be derived from (2.16) and (2.19) and is

$$\left(K_0 + \frac{1}{2}F\eta_0^2\right)_t + G_{0x}^{(x)} + G_{0y}^{(y)} = 0, \tag{2.25a}$$

where

$$G_0^{(x)} = u_0K_0 + (u_1 + \eta_{1y})\eta_0 - u_0\eta_0\epsilon^{-1}h_B, \tag{2.25b}$$

$$G_0^{(y)} = v_0K_0 + (v_1 - \eta_{1x})\eta_0 - v_0\eta_0\epsilon^{-1}h_B, \tag{2.25c}$$

and where $(u_1 + \eta_{1y})$ and $(v_1 - \eta_{1x})$ in (2.25b, c) may be found in terms of η_0 from (2.16a, b).

Initial-value problems require the specification at $t = 0$ of $\eta_0(x, y, 0)$. At rigid boundaries the no-normal-flow condition of the SWE translates in the QG approximation to the requirement that

$$\eta_0 = C_j(t), \tag{2.26}$$

for each connected boundary $j = 1, 2, \cdots$, where the C_j are determined so that the integral constraints corresponding to conservation of mass and the conservation of circulation around each boundary are maintained (McWilliams 1977).

3. Intermediate models

A number of different intermediate models for the f-plane SWE are described in this section. To achieve the objective of representing small Rossby number flows with $O(1)$ variations in $h = \epsilon F\eta + 1 - h_B$, which may result either from $O(1)$ variations in the bottom topographic height h_B or in the interface displacement $\epsilon F\eta$, most of the intermediate models below retain the full continuity equation (2.1a). The need to include the complete representation of h in (2.1a) is clear from the objective, and this in turn implies limitations on approximations that may be made in (2.1a) for u and v. For example, consider the continuity equation (2.1a) written in the form

$$\epsilon F\eta_t + uh_x + vh_y + hD = 0, \tag{3.1}$$

as in the derivation of the QG approximation. If h is represented in all terms by (2.1d), then expressions for u and v that include the divergent parts that contribute to D must be retained in uh_x and vh_y to conserve mass properly, i.e., so that the differentiated terms in (3.1) can be recombined and the divergence form of (2.1a) restored. The use of (2.1a) implies that a boundary condition at rigid walls consistent with conservation of mass is that the normal component of the velocity (u, v) vanish.

It should be noted that, in general, intermediate models may involve no more formal accuracy in Rossby number ϵ than the quasi-geostrophic approximation (McWilliams and Gent 1980). The properties of the intermediate models concerning the conservation of potential vorticity on fluid particles and conservation

of energy and potential enstrophy are summarized in Table 1. In addition, the equations for the models are summarized by expressing them in a common formulation in appendix C.

a. *Intermediate model—IM*

This intermediate model is probably the closest to QG in that it is based on similar momentum equations, but unlike QG utilizes the full continuity equation. It is obtained by iteration of the momentum equations (2.1b, c) written in the form,

$$u = -\eta_y - \epsilon(uv_x + vv_y) - \epsilon v_t, \quad (3.2a)$$

$$v = \eta_x + \epsilon(uu_x + vu_y) + \epsilon u_t, \quad (3.2b)$$

using

$$u_G = -\eta_y, \quad v_G = \eta_x, \quad (3.3a,b)$$

as a first approximation in the $O(\epsilon)$ terms on the right-hand side. The resulting approximate momentum equations are,

$$\epsilon u_{Gt} - \epsilon\zeta_G v_G - v = -\mathcal{B}_{Gx}, \quad (3.4a)$$

$$\epsilon v_{Gt} + \epsilon\zeta_G u_G + u = -\mathcal{B}_{Gy}, \quad (3.4b)$$

where

$$\zeta_G = v_{Gx} - u_{Gy} = \nabla^2\eta, \quad (3.4c)$$

$$\mathcal{B}_G = \eta + \epsilon K_G, \quad K_G = \tfrac{1}{2}(u_G^2 + v_G^2). \quad (3.4d,e)$$

In this intermediate model and in many of those that follow, we assume that the adopted momentum equations, such as (3.4a, b), provide the defining relations for approximate values of (u, v) that are retained in the continuity equation (2.1a).

The vorticity equation implied by (3.4) is

$$\epsilon(\zeta_{Gt} + u_G\zeta_{Gx} + v_G\zeta_{Gy}) + D = 0. \quad (3.5)$$

A single equation for η may be obtained by substituting the expressions for u and v from (3.4a, b) in the continuity equation (2.1a) (e.g., Williams 1985; Cushman-Roisin 1986; Hukuda and Yamagada 1988):

$$(h\eta_{xt})_x + (h\eta_{yt})_y - F\eta_t = -\epsilon^{-1}J(h, \mathcal{B}_G) - J(\eta, h\zeta_G). \quad (3.6)$$

Boundary conditions for (3.6) on η at solid walls may be obtained by using (3.4) to determine the normal component of velocity (u, v) and by setting that equal to zero. In the numerical solutions in Parts II and III, (3.6) is regarded essentially as a linear equation in η_t with η known. Since $h > 0$, $F\eta_t$ and the highest derivative terms $h\nabla^2\eta_t$ retain opposite signs which implies, with appropriate boundary conditions, the existence of a unique solution for η_t (e.g., Garabedian 1964, Chaps. 7, 8).

A disadvantage of this model is that conservation statements, corresponding to those for potential vorticity (2.6) or energy (2.11) in the SWE, have not been found. The relation of IM to the linear balance equations (LBE) (e.g., Gent and McWilliams 1983a) is discussed in section 3f.

For comparison with results from other models, it is useful to note that if the approximate momentum equations (3.4) of IM are used to obtain an estimate for an $O(\epsilon)$ correction to the geostrophic vorticity by forming a divergencc equation, we find

$$\zeta = \zeta_{HV} = \zeta_G - \epsilon 2J(u_G, v_G). \quad (3.7)$$

We mention that the governing equation (2.23) for QG may be derived in a manner similar to that used to obtain (3.6) for IM by substituting u and v from (3.4a,b) in the following approximate form of the continuity equation (2.3a):

$$\epsilon F\eta_t + (\hat{H}u_G)_x + (\hat{H}v_G)_y + D = 0. \quad (3.8)$$

In the QG approximation $\hat{H} = O(\epsilon)$ and from (3.4) $D = O(\epsilon)$, so that all of the leading order terms are consistently retained in (3.8).

b. *Geostrophic vorticity—GV*

Advection of geostrophic vorticity by u and v and the consequent conservation of geostrophic potential vorticity is insured here by finding approximate expressions for u and v from iteration of the momentum equations as written in (2.3b, c), i.e., from

$$u = (1 + \epsilon\zeta)^{-1}(-\mathcal{B}_y - \epsilon v_t), \quad (3.9a)$$

$$v = (1 + \epsilon\zeta)^{-1}(\mathcal{B}_x + \epsilon u_t), \quad (3.9b)$$

TABLE 1. Properties of the shallow water equations, the quasi-geostrophic equations, and the intermediate models with regard to the existence (marked by a check) of analogues of potential vorticity conservation on fluid particles and to the conservation of energy.

Model	Potential vorticity*	Energy
SWE	✓	✓
QG	✓	✓
IM		
GV	✓	
GM	✓	✓
HP	✓	✓
BE	✓	
LBE		
LQBE	✓	
HBE		
BEM	✓	
NBE	✓	
SE	✓	
MSE		

* All models (except SE; see section 3k) that have analogues of potential vorticity conservation on fluid particles have corresponding conservation equations for potential enstrophy, e.g., (2.8), (2.24), and (3.13).

where the iteration is carried out separately in the numerator and in the denominator. This corresponds to retaining the full u and v in the rotation terms in (2.3). The resulting approximate momentum equations are

$$\epsilon u_{Gt} - (\epsilon\zeta_G + 1)v = -\mathcal{B}_{Gx}, \quad (3.10a)$$

$$\epsilon v_{Gt} + (\epsilon\zeta_G + 1)u = -\mathcal{B}_{Gy}. \quad (3.10b)$$

The vorticity equation

$$\epsilon(\zeta_{Gt} + u\zeta_{Gx} + v\zeta_{Gy}) + (\epsilon\zeta_G + 1)D = 0, \quad (3.11)$$

follows from (3.10a, b). The combination of (3.11) and (2.1a) gives

$$Q_{Gt} + uQ_{Gx} + vQ_{Gy} = 0, \quad (3.12a)$$

which implies the conservation of geostrophic potential vorticity

$$Q_G = (1 + \epsilon\zeta_G)/h, \quad (3.12b)$$

following fluid particles moving with velocities (u, v) (3.10). The combination of (3.12a) and (2.1a) yields an equation for the conservation of geostrophic potential enstrophy hQ_G^2,

$$(hQ_G^2)_t + (huQ_G^2)_x + (hvQ_G^2)_y = 0. \quad (3.13)$$

A potential enstrophy conservation law will follow in general for the subsequent intermediate models that retain (2.1a) and that conserve some approximate form of potential vorticity following fluid particles as in (3.12).

One equation for η is obtained by substituting u and v from (3.10) in (2.1a):

$$(h_G\eta_{xt})_x + (h_G\eta_{yt})_y - F\eta_t = -\epsilon^{-1}J(h_G, \mathcal{B}_G), \quad (3.14a)$$

where

$$h_G = h/(1 + \epsilon\zeta_G). \quad (3.14b)$$

Boundary conditions for (3.14) on η at solid walls may be obtained by using (3.10) and setting the normal component of (u, v) equal to zero. Similar to IM, (3.14a) is regarded as a linear equation in η_t in the numerical solution procedure. The condition $(1 + \epsilon\zeta_G) > 0$ implies $h_G > 0$ and ensures the retention of opposite signs on the terms $F\eta_t$ and $h_G\nabla^2\eta_t$.

An equation expressing the conservation of energy has not been found for this model. The GV model was formulated and applied by Sutyrin and Yushina [1986a,b; 1988]. The approximation (3.10) on which GV is based was also mentioned briefly by Schär and Davies (1988).

c. *Geostrophic momentum—GM*

The geostrophic momentum approximation was described by Hoskins (1975) and attributed there to Eliassen (1948). It has been widely applied to studies of atmospheric motion (e.g., Hoskins 1982) where it is frequently employed in conjunction with a transformation to geostrophic coordinates, after which the model is referred to as the semigeostrophic equations.

In GM, advection of momentum, assumed to be represented by the geostrophic values u_G and v_G, by the full u and v velocities is retained so that (2.1b, c) are approximated by

$$\epsilon(u_{Gt} + uu_{Gx} + vu_{Gy}) - v = -\eta_x, \quad (3.15a)$$

$$\epsilon(v_{Gt} + uv_{Gx} + vv_{Gy}) + u = -\eta_y. \quad (3.15b)$$

Separate expressions for u and v may be obtained by algebraic manipulation of (3.15):

$$u = (1 + \epsilon\zeta_{GM})^{-1}[-\mathcal{B}_{Gy} - \epsilon v_{Gt} + \epsilon^2(u_{Gy}v_{Gt} - v_{Gy}u_{Gt})], \quad (3.16a)$$

$$v = (1 + \epsilon\zeta_{GM})^{-1}[\mathcal{B}_{Gx} + \epsilon u_{Gt} + \epsilon^2(v_{Gx}u_{Gt} - u_{Gx}v_{Gt})], \quad (3.16b)$$

where

$$\zeta_{GM} = \zeta_G + \epsilon J(u_G, v_G). \quad (3.17)$$

An equation for ζ_{GM} follows directly from (3.16) by forming D from u and v:

$$\epsilon(\zeta_{GMt} + u\zeta_{GMx} + v\zeta_{GMy}) + (\epsilon\zeta_{GM} + 1)D = 0. \quad (3.18)$$

The combination of (3.18) and (2.1a) gives

$$Q_{GMt} + uQ_{GMx} + vQ_{GMy} = 0, \quad (3.19a)$$

which expresses the conservation of geostrophic momentum potential vorticity

$$Q_{GM} = (1 + \epsilon\zeta_{GM})/h, \quad (3.19b)$$

following fluid particles moving with velocities (u, v) (3.16).

A single equation for η is obtained by substituting (3.16a, b) in (2.1a):

$$(h_{GM}\eta_{xt})_x + (h_{GM}\eta_{yt})_y - F\eta_t + \epsilon J(\eta_x, h_{GM}\eta_{yt}) - \epsilon J(\eta_y, h_{GM}\eta_{xt}) = -\epsilon^{-1}J(h_{GM}, \mathcal{B}_G), \quad (3.20a)$$

where

$$h_{GM} = h/(1 + \epsilon\zeta_{GM}). \quad (3.20b)$$

Again, the zero normal flow boundary condition on (u, v) may be expressed in terms of η by utilizing (3.16). Also, (3.20a) regarded as a linear equation for η_t is elliptic as long as $(1 + \epsilon\zeta_{GM}) > 0$.

The GM model, (3.15a, b) and (2.1a), possesses the energy conservation equation

$$\epsilon\left(hK_G + \frac{1}{2}F\eta^2\right)_t + (uh\mathcal{B}_G)_x + (vh\mathcal{B}_G)_y = 0. \quad (3.21)$$

If a divergence equation is formed from the GM approximate momentum equations (3.15), we obtain

$$\zeta = \zeta_G - \epsilon 2[J(u, v_G) + J(u_G, v)]. \quad (3.22)$$

which to $O(\epsilon)$ is equivalent to (3.7) for ζ_{HV}. It is curious

that the $O(\epsilon)$ corrections to ζ_G in ζ_{HV} and in ζ_{GM} involve the same function $J(u_G, v_G)$, but that they differ in sign and magnitude. An implication of the difference between (3.17) and (3.22) is that the geostrophic momentum vorticity ζ_{GM} in Q_{GM} differs at $O(\epsilon)$ from the vorticity (3.22) of the advection velocities in the equation (3.19) for Q_{GM} with error $|\zeta - \zeta_{GM}| > |\zeta - \zeta_G|$.

d. Salmon's equation—HP

Salmon (1983) has derived a set of approximate equations for nearly geostrophic flow in a fluid governed by the shallow-water equations in an original manner by making approximations in the Lagrangian before applying Hamilton's Principle. Approximations in the Lagrangian that do not break time and particle-label symmetries are utilized and, as a result, the derived approximate equations conserve analogues of total energy and potential vorticity (see also Salmon 1985, 1988a,b). The procedure of Salmon (1983) is followed in appendix A to obtain approximations to the SWE when bottom topographic variations are present. The resulting momentum equations are

$$\epsilon u_{Gt} - (\epsilon\zeta_G + 1)v = -\mathcal{B}_{HPx}, \quad (3.23a)$$

$$\epsilon v_{Gt} + (\epsilon\zeta_G + 1)u = -\mathcal{B}_{HPy}, \quad (3.23b)$$

where

$$\mathcal{B}_{HP} = \eta + \frac{1}{2}\epsilon(u_G^2 + v_G^2 + \epsilon 2u_G u_A + \epsilon 2v_G v_A) + (\epsilon/F)h\zeta_A - (\epsilon/F)(-u_A h_{By} + v_A h_{Bx}), \quad (3.23c)$$

$$\zeta_A = v_{Ax} - u_{Ay}, \quad (3.23d)$$

$$u = u_G + \epsilon u_A, \quad v = v_G + \epsilon v_A. \quad (3.24a,b)$$

For $h_B = 0$, (3.23) are equivalent to Salmon's (1983) equations (4.6).

The vorticity equation for ζ_G is the same as (3.11) in GV and again (3.11) and (2.1a) may be combined to imply the conservation of geostrophic potential vorticity Q_G (3.12). The resulting equation expressing energy conservation is discussed in appendix A. For the solution of (3.23) and (2.1a), it is necessary to utilize diagnostic equations, e.g., those for u_A and v_A (A13a, b) which are derived in appendix A.

For comparison with the other models and for use in section 4, we substitute u and v from (3.23) in (2.1a) to obtain

$$(h_G\eta_{xt})_x + (h_G\eta_{yt})_y - F\eta_t = -\epsilon^{-1}J(h_{GV}, \mathcal{B}_{HP}). \quad (3.25)$$

In this case (3.25) is not an equation for η alone, since $\mathcal{B}_{HP}$ (3.23c) depends on u_A and v_A and those variables are obtained from the solution of the diagnostic equations (A13a, b). Boundary conditions are discussed in appendix A.

Note that the difference between this model and GV is represented by the difference between $\mathcal{B}_{HP}$ (3.23c) and $\mathcal{B}_G$ (3.4d) as may be seen by a comparison of the momentum equations (3.23) and (3.9) or of (3.25) and (3.14a). Evidently, it is the presence of the additional terms in $\mathcal{B}_{HP}$ that results in energy conservation in HP.

e. Balance equations—BE

The balance equations (Charney 1955, 1962; Bolin 1955, 1956; Gent and McWilliams 1983a) are obtained by a procedure that is different than that used for the previous models. In this case, the velocity components are written as the sum of rotational and divergent components,

$$u = -\psi_y + \epsilon\chi_x, \quad v = \psi_x + \epsilon\chi_y, \quad (3.26a,b)$$

so that

$$\zeta = v_x - u_y = \nabla^2\psi, \quad (3.27)$$

$$D = u_x + v_y = \epsilon\nabla^2\chi. \quad (3.28)$$

The governing equations, in addition to the continuity equation (2.1a), are obtained from the vorticity (2.4) and divergence equations (2.5) by substituting for u and v from (3.26) and retaining $O(1)$ and $O(\epsilon)$ terms. For the shallow-water equations, this results in retention of all the terms in the vorticity equation (2.4),

$$\zeta_t + u\zeta_x + v\zeta_y + (1 + \epsilon\zeta)\nabla^2\chi = 0, \quad (3.29)$$

and, from (2.5), in an approximate divergence or balance equation,

$$\zeta = \nabla^2\psi = \nabla^2\eta - \epsilon 2J(\psi_x, \psi_y). \quad (3.30)$$

The approximate governing equations are then (2.1a), (3.29) and (3.30). The vorticity equation (3.29) combines with (2.1a) to give the conservation of potential vorticity following fluid particles moving with velocity (u, v) (3.26) as in (2.6). To insure consistency of (2.1a), (3.29) and (3.30), an omega equation, derived by substituting (3.29) and ∇^2 (2.1a) in the time derivative of (3.30),

$$\nabla^2 D - FD = \epsilon F(u\zeta_x + v\zeta_y + \epsilon\zeta\nabla^2\chi) - \nabla^2[(\hat{H}u)_x + (\hat{H}v)_y] - 2\epsilon^2 FJ(\psi_x, \psi_y)_t, \quad (3.31)$$

is frequently used in place of either (2.1a) or (3.29) in numerical solution procedures (Gent and McWilliams 1983a; Norton et al. 1986).

An alternate solution procedure, which we briefly outline in appendix B, utilizes (2.9) for Q_L, (3.29) and (3.30). In fact, most of the intermediate models discussed here, as well as QG, can be formulated in a manner similar to this. A summary is given in appendix C.

No equation expressing energy conservation has been found for BE applied to the SWE (Gent and McWilliams 1984). Note that this situation differs from BE in the continuously stratified case where, in periodic

domains with a rigid lid and no topography, energy is conserved (Lorenz 1960), but potential vorticity on fluid particles is not. We note that for the shallow-water equations, BE and QG are potential vorticity conserving models that have in common the property that the relative vorticity in the approximate potential vorticity Q is derived from the advection velocities in the equation for Q (LQBE and BEM, sections 3g and 3i, also have this property). In addition, BE and BEM are the only models for which the relative vorticity in the conserved Q is exactly that given by the implied divergence, or balance equation (see appendix C). The momentum equations that correspond to the truncation of the vorticity and divergence equations in BE do not follow directly from (2.1b, c), but involve implicitly defined force potential correction terms and are referred to as the equivalent momentum equations (Gent and McWilliams 1983a). Methods to obtain numerical finite-difference solutions of BE are described in Norton et al. (1986), appendix B, and in Parts II and III. Application of boundary conditions at rigid walls is discussed in Gent and McWilliams (1983a) and in Part III.

f. Linear balance equations—LBE

In LBE (Gent and McWilliams 1983a) the velocity components are represented as in (3.26), but only O(1) terms are retained in the approximate divergence equation (3.30) so that the equation of balance is linear,

$$\nabla^2\psi = \nabla^2\eta, \tag{3.32}$$

which implies, for our f-plane problems,

$$\psi = \eta. \tag{3.33}$$

Likewise, only lowest order terms are retained in the vorticity equation which with (3.33) is

$$\zeta_{Gt} + u_G\zeta_{Gx} + v_G\zeta_{Gy} + \nabla^2\chi = 0, \tag{3.34}$$

where u_G, v_G, and ζ_G are defined in (3.3) and (3.4c). The continuity equation (2.1a) becomes

$$\epsilon F\eta_t + [(u_G + \epsilon\chi_x)\hat{H}]_x + [(v_G + \epsilon\chi_y)\hat{H}]_y + \epsilon\nabla^2\chi = 0. \tag{3.35}$$

The governing equations are then (3.34) and (3.35). The LBE have no relations expressing conservation of potential vorticity or energy. Solution procedures are discussed in Part II.

As in BE, implicitly defined terms in equivalent momentum equations are required for consistency with (3.32) and (3.34) (Gent and McWilliams 1983a). We note, however, that since LBE are governed by (3.34) and (3.35), we may assume alternatively that the approximate momentum equations (3.4) for IM [which imply (3.34)] hold, while (2.1a) is separately approximated by (3.35). This procedure is similar to the method used in connection with (3.8) to obtain QG. With this formulation, (3.32) is only a leading order approximation to the balance equation (3.7) implied by (3.4), as is the case in QG and IM, and the $O(\epsilon)$ correction term in (3.7) is assumed to be balanced by a streamfunction correction rather than an implied force potential. Because of the similarity with the QG and IM models, we prefer the interpretation of the LBE model (3.34) and (3.35) based on the approximate momentum equations (3.4) and will utilize that in the subsequent discussions.

Note that the vorticity equation (3.34) in LBE is similar to that in IM (3.5) and both models use (2.1a). The approximations differ, however, in that for LBE the u and v in (3.35) have vorticity ζ_G, whereas in IM the u and v in (2.1a) have vorticity ζ_{HV}(3.7). [Compare also (C5) and (C10).]

g. Linear balance equations (potential vorticity conserving)—LQBE

We point out that a model similar to LBE and GV that conserves potential vorticity may be constructed by retaining some of the $O(\epsilon)$ terms in the vorticity equation (3.29) which becomes

$$\zeta_{Gt} + (u_G + \epsilon\chi_x)\zeta_{Gx} + (v_G + \epsilon\chi_y)\zeta_{Gy} + (1 + \epsilon\zeta_G)\nabla^2\chi = 0. \tag{3.36}$$

Thus, LQBE is governed by (3.35) and (3.36). These imply

$$Q_{Gt} + (u_G + \epsilon\chi_x)Q_{Gx} + (v_G + \epsilon\chi_y)Q_{Gy} = 0, \tag{3.37}$$

so that Q_G is conserved on particles moving with velocities $(u_G + \epsilon\chi_x, v_G + \epsilon\chi_y)$. We have found no equation expressing conservation of energy for LQBE. Similar to LBE, we may assume that approximate momentum equations are

$$\epsilon u_{Gt} - \epsilon\zeta_G(v_G + \epsilon\chi_y) - v = -\mathcal{B}_{Gx}, \tag{3.38a}$$

$$\epsilon v_{Gt} + \epsilon\zeta_G(u_G + \epsilon\chi_x) + u = -\mathcal{B}_{Gy}, \tag{3.38b}$$

which imply (3.36). Procedures for obtaining numerical solutions and applying wall boundary conditions are discussed in Parts II and III.

h. Hybrid balance equations—HBE

We have noticed that an additional set of models (HBE, BEM, NBE) based on approximations similar to those involved in the formulation of BE may be derived directly from approximate momentum equations. These models are of interest because of the possibility that the existence of approximate momentum equations might help clarify the formulation of consistent boundary conditions at rigid walls (Part III).

In HBE, approximate momentum balances are obtained by substituting (3.26) in (2.3b,c) and retaining $O(\epsilon)$ terms. Using the notation

$$u_R = -\psi_y, \quad v_R = \psi_x, \tag{3.39a,b}$$

we obtain

$$\epsilon u_{Rt} - \epsilon\zeta v_R - v = -\mathcal{B}_{Rx}, \quad (3.40a)$$

$$\epsilon v_{Rt} + \epsilon\zeta u_R + u = -\mathcal{B}_{Ry}, \quad (3.40b)$$

where

$$\mathcal{B}_R = \eta + \frac{\epsilon}{2}(u_R^2 + v_R^2). \quad (3.40c)$$

The vorticity equation, implied by (3.40) is

$$\epsilon(\zeta_t + u_R\zeta_x + v_R\zeta_y) + D = 0, \quad (3.41)$$

while the divergence equation formed from (3.40) reduces exactly to the equation of balance,

$$\zeta = \nabla^2\psi = \nabla^2\eta - \epsilon 2J(\psi_x, \psi_y). \quad (3.42)$$

The governing equations for HBE are then (3.41), (3.42), and (2.1a), with velocity components defined by (3.26) and (3.39).

Numerical finite difference solutions of HBE may be obtained by methods similar to those used for BE (Norton et al. 1986; Part II). An alternative solution procedure may be formulated by using the momentum equations and substituting u and v from (3.40) in (2.1a), which gives

$$(h\psi_{xt})_x + (h\psi_{yt})_y - F\eta_t = -\epsilon^{-1}J(h, \mathcal{B}_R) - J(\psi, h\zeta_R). \quad (3.43)$$

Equations (3.42) and (3.43) form two coupled governing equations for ψ and η. Numerical finite difference solutions of (3.42) and (3.43) are found for doubly periodic domains in Part II. In that case, the variable χ, which has been eliminated from (3.42) and (3.43), does not have to be found explicitly. Aspects of this solution procedure are discussed in appendix B.

No conservation statements for potential vorticity or for energy have been found for HBE. Note that HBE may be considered as an extension of IM, with the difference between the two being the inclusion in HBE of the $O(\epsilon)$ term in the balance equation (3.42). If that term is dropped, such that $\nabla^2\psi = \nabla^2\eta$ and $\psi = \eta$, HBE reduces to IM. Although the HBE model does not have potential vorticity conservation, it does have approximate momentum equations which imply the balance equation (3.42) exactly. Consequently, we thought that it would be useful to evaluate the accuracy of HBE in Part II to help clarify the importance in an intermediate model of retaining the balance equation (3.42) (by comparison of HBE with IM) and of possessing potential vorticity conservation (by comparison of HBE with BE).

i. Balance equations (based on momentum equations)—BEM

A model very close to BE may be derived from (2.1a) and the following approximate momentum equations:

$$\epsilon u_{Rt} - (\epsilon\zeta + 1)v = -\mathcal{B}_{Rx}, \quad (3.44a)$$

$$\epsilon v_{Rt} + (\epsilon\zeta + 1)u = -\mathcal{B}_{Ry}. \quad (3.44b)$$

These are similar to (3.40) for HBE with the exception that the full u and v are retained here in the rotation terms. The vorticity equation (3.29) follows from (3.44a, b) and (3.29) combines with (2.1a) to give conservation of potential vorticity (2.6) on fluid particles moving with velocity (3.26), as in BE.

The governing equations are thus (2.1a), (3.29), and the equation of balance,

$$\zeta = \nabla^2\psi = \nabla^2\eta - \epsilon 2J(\psi_x, \psi_y) - \epsilon^2 J(\zeta, \chi), \quad (3.45)$$

which follows from (3.44a, b). The only difference between BEM and BE is the inclusion of the extra $O(\epsilon^2)$ terms in (3.45) compared to (3.30). No relation expressing conservation of energy has been found for BEM. Numerical finite difference solution procedures for BEM are discussed in appendix B and Part II. Application of wall boundary conditions is discussed in Part III.

j. Near balance equations—NBE

The NBE model utilizes momentum equations similar to (3.44a, b) for BEM with the exception that the streamfunction is expanded as

$$\psi = \psi_0 + \epsilon^2\psi_1, \quad (3.46)$$

and we assume

$$\epsilon u_{R0t} - (1 + \epsilon\zeta_{R0})v = -\mathcal{B}_{R0x}, \quad (3.47a)$$

$$\epsilon v_{R0t} + (1 + \epsilon\zeta_{R0})u = -\mathcal{B}_{R0y}, \quad (3.47b)$$

where

$$u_{R0} = -\psi_{0y}, \quad v_{R0} = \psi_{0x}, \quad (3.48a,b)$$

$$\zeta_{R0} = \nabla^2\psi_0, \quad \mathcal{B}_{R0} = \eta + \frac{1}{2}\epsilon(u_{R0}^2 + v_{R0}^2). \quad (3.48c,d)$$

The equation of balance,

$$\nabla^2\psi_0 = \nabla^2\eta - \epsilon 2J(\psi_{0x}, \psi_{0y}), \quad (3.49)$$

which follows from approximating the divergence equation found from (3.47) to $O(\epsilon)$ is also assumed to hold.

The vorticity equation implied by (3.47) is

$$\epsilon(\zeta_{R0t} + u\zeta_{R0x} + v\zeta_{R0y}) + (\epsilon\zeta_{R0} + 1)D = 0, \quad (3.50)$$

which combines with (2.1a) to give

$$Q_{R0t} + uQ_{R0x} + vQ_{R0y} = 0, \quad (3.51a)$$

expressing the conservation of NBE potential vorticity

$$Q_{R0} = (1 + \epsilon\zeta_{R0})/h, \quad (3.51b)$$

following fluid particles moving with velocities (u, v) (3.47).

Substitution of u and v from (3.47) and (2.1a) gives

$$(h_{R0}\psi_{0xt})_x + (h_{R0}\psi_{0yt})_y - F\eta_t = -\epsilon^{-1}J(h_{R0}, \mathcal{B}_{R0}), \quad (3.52a)$$

where

$$h_{R0} = h/(1 + \epsilon\zeta_{R0}). \quad (3.52b)$$

Similar to (3.42) and (3.43) for HBE, (3.49) and (3.52) form two coupled governing equations for η and ψ_0. Numerical solutions to these equations for flow in doubly periodic domains are presented in Part II where, as with HBE, the variable χ does not have to be calculated. Aspects of the solution procedure are discussed in appendix B. Boundary conditions for solid walls are discussed in Part III. We will assume in subsequent discussions that these boundary conditions, and those for BE, HBE, and BEM, are such that for the limit $\epsilon \to 0$ the reduction of the equations of balance (3.30), (3.42), (3.45), and (3.49) to $\nabla^2\psi = \nabla^2\eta$ implies $\psi = \eta$.

As is the case for the BE, no equation expressing energy conservation has been found for NBE. Note that this derivation of NBE follows the same idea as that used for GV with an additional $O(\epsilon)$ correction from (3.49) retained in ψ_0 here. If we expand $\psi = \psi_0 + \epsilon\psi_1$ in place of (3.46) so that (3.49) becomes $\nabla^2\psi_0 = \nabla^2\eta$ and $\psi_0 = \eta$, NBE reduces to GV.

k. *Slow equations—SE*

Using ideas of normal mode initialization, Lynch (1989) has recently derived a set of approximate equations to model low frequency atmospheric motions. His derivation is applied to the shallow water equations, which are represented by equations for the divergence D (2.5), the potential vorticity Q (2.6), and by an additional equation,

$$\epsilon FI_t + \nabla^2 D - FD = \epsilon F[(u\zeta)_x + (v\zeta)_y] - \nabla^2[(\hat{H}u)_x + (\hat{H}v)_y], \quad (3.53)$$

for the geostrophic imbalance,

$$I = \nabla^2\eta - \zeta, \quad (3.54)$$

where (3.53) follows from combining ∇^2 (2.1a) and F (2.4). In addition, the derivation procedure utilizes (2.9) for Q_L, the linearized potential vorticity.

Considering linear approximations to (2.5), (2.9), and (3.53), Lynch (1989) argues that, since slow (low-frequency rotational) modes are time-independent, geostrophic and nondivergent while fast (high-frequency gravity wave) modes have zero linearized potential vorticity, the time derivatives of D and I project onto the fast modes and the time derivative of Q_L projects onto the slow modes. Thus, approximate equations are derived by dropping the time derivatives of D and I (associated in the linear limit with the fast modes) in (2.5) and (3.53), respectively, and by retaining the full potential vorticity equation (2.6). The resulting slow equation (SE) are

$$\zeta = \nabla^2\eta - \epsilon 2J(u, v) + \epsilon[(uD)_x + (vD)_y], \quad (3.55)$$

$$\nabla^2 D - FD = \epsilon F[(u\zeta)_x + (v\zeta)_y] - \nabla^2[(\hat{H}u)_x + (\hat{H}v)_y], \quad (3.56)$$

and (2.6). Methods for solving the SE numerically are outlined in Lynch (1989) and are also given in Part II, where a decomposition of the velocity components u and v into rotational and divergent parts as in (3.26) is utilized. The neglect of D_t in (3.55) results in an equation of balance, similar to (3.30) in BE, but with more terms retained. The neglect of I_t in (3.56) results in an equation somewhat similar in form to the omega equation (3.31) in BE, but with the last term in (3.31) absent in (3.56).

There is a basic difference between SE and the intermediate models discussed previously in that the full continuity equation (2.1a) is not retained in SE. This is a result of the fact that (3.55) and (3.56) are not consistent with (2.1a) and (2.4). We note that equivalent continuity and vorticity equations for SE that are consistent with the conservation of potential vorticity (2.6) may be written in the form,

$$\epsilon F\eta_t + (u\hat{H})_x + (v\hat{H})_y + D + hD' = 0, \quad (3.57)$$

$$\epsilon[\zeta_t + (u\zeta)_x + (v\zeta)_y] + D + (1 + \epsilon\zeta)D' = 0, \quad (3.58)$$

where we use the notation

$$D' = u'_x + v'_y, \quad (3.59)$$

and where the total velocity components here are designated by

$$u_T = u + u', \quad v_T = v + v'. \quad (3.60a,b)$$

Equations (3.57) and (3.58) may be derived from (2.1a) and (2.4) by using the velocity components (3.60) and neglecting certain terms. We have not found corresponding consistent momentum equations that imply (3.58), however.

An equation for D' follows from the requirement that (3.57) and (3.58) be consistent also with (3.55) and (3.56). Substituting ∇^2 (3.57) and F (3.58) in the time derivative of ϵF (3.55) and then subtracting (3.56), we obtain

$$\nabla^2(hD') - (1 + \epsilon\zeta)D' = \epsilon^2 F[2J(u, v) - (uD)_x - (vD)_y]_t. \quad (3.61)$$

A nonzero value for the right hand side of (3.61) may be expected in general and that will require the existence of $D' \neq 0$. A nonzero value of D' implies that the flux terms in the equivalent continuity equation (3.57) are not in divergence form and that mass is not necessarily conserved locally. To assess the global conservation of mass, we consider solutions in doubly pe-

riodic domains. From the area integral of (3.57) over the domain, we obtain

$$\epsilon F \iint \eta_t dxdy = -\iint hD'dxdy. \quad (3.62)$$

Although in the numerical solution procedure in Part II, it is not necessary to calculate D' explicitly or to consider (3.61), the numerical results confirm through nonzero values of the left hand side of (3.62), that $D' \neq 0$. Thus, the SE do not necessarily conserve mass globally either.

Note also that although the SE model conserves potential vorticity on fluid particles (2.6), because of the implied approximation (3.57) to the continuity equation, a conservation equation for potential enstrophy similar to (2.8) does not exist. On the other hand, we note that the area integral of (3.61) over the doubly periodic domain gives

$$\iint (1 + \epsilon\zeta)D'dxdy = 0, \quad (3.63)$$

which from (3.58) implies

$$\iint \zeta_t dxdy = 0, \quad (3.64)$$

so that this property of the SWE implied by (2.4) is preserved. No statement expressing energy conservation has been found.

The relaxation in SE of the requirement that the full continuity equation (2.1a) be retained is a marked departure from the other intermediate models that utilize (2.1a). We thought this different feature of SE made it an interesting model to include in the evaluations involving numerical solutions in doubly periodic domains in Part II. The failure of SE to conserve mass globally, however, seems to be a potentially troublesome property. In addition, the lack of readily identifiable approximate momentum equations makes some applications, including those in section 6, difficult. Because of these drawbacks, we omit SE from further discussion here, but include some numerical results in Part II. In order to retain a model that is based on the same idea, however, we follow Lynch's (1989) procedure and formulate a set of modified slow equations (MSE) that conserve mass globally as described in the next section.

l. Modified slow equations—MSE

For this model, the procedure utilized by Lynch (1989) in deriving the SE is followed with the exception that (2.9) for Q_L is retained rather than (2.6) for Q. The MSE thus consist of (3.55), (3.56) and (2.9). We remark that the retention of (2.9) seems to be at least as consistent with the rationale for the derivation of SE, based on linear wave modes, as is the retention of (2.6). Numerical solution procedures and results for MSE are presented in Part II.

Similar to SE, we can identify equivalent continuity and vorticity equations for MSE that are consistent with (2.9) and that follow as approximations to (2.1a) and (2.4). These are

$$\epsilon F\eta_t + (u\hat{H})_x + (v\hat{H})_y + D + D' = 0, \quad (3.65)$$

$$\epsilon[\zeta_t + (u\zeta)_x + (v\zeta)_y] + D + D' = 0, \quad (3.66)$$

where the notation (3.59) and the definitions (3.60) are again utilized. In this case, it is also useful to represent u and v in terms of ψ and χ as in (3.26) so that (3.27) and (3.28) hold and further to define

$$u' = \epsilon\chi'_x, \quad v' = \epsilon\chi'_y, \quad (3.67a,b)$$

so that

$$D' = \epsilon\nabla^2\chi'. \quad (3.68)$$

Moreover, we can identify approximate momentum equations,

$$-\epsilon\psi_{yt} - \epsilon\zeta v - v_T = -\mathcal{B}_x, \quad (3.69a)$$

$$\epsilon\psi_{xt} + \epsilon\zeta u + u_T = -\mathcal{B}_y, \quad (3.69b)$$

where $\mathcal{B}$ is defined as in (2.3d), that imply both the equivalent vorticity equation (3.66) and the MSE equation of balance (3.55).

An equation for D' follows from the requirement that (3.65) and (3.66) be consistent with (3.55) and (3.56). Substituting ∇^2 (3.65) and F (3.66) in the time derivative of (3.55) and subtracting (3.56), we obtain

$$\nabla^2 D' - FD' = \epsilon^2 F[2J(u, v) - (uD)_x - (vD)_y]_t. \quad (3.70)$$

As in (3.61) for SE, a nonzero value for the terms on the right hand side of (3.70) will imply $D' \neq 0$. In MSE, however, the flux terms in the equivalent continuity equation (3.65) are written in divergence form and mass is conserved globally. The area integrals over a doubly periodic domain of (3.65) and (3.66) give (3.64) and

$$\iint \eta_t dxdy = 0, \quad (3.71)$$

as in the SWE.

The MSE do not conserve potential vorticity on fluid particles exactly and a conservation law for energy has not been found.

4. Limiting cases

All of the intermediate models discussed in section 3 (except SE) and QG are given in a common formulation in appendix C. The behavior of the intermediate models in the relevant limiting cases of quasi-geostrophic flow and linear ageostrophic coast-

ally trapped waves may be readily found from this formulation.

a. Quasi-geostrophic limit

For the limit $\epsilon \to 0$, $\hat{h}_B = \epsilon^{-1}h_B = O(1)$, $F = O(1)$, and with η expanded as in (2.13), all of the intermediate models in appendix C reduce to the QG (2.23) [or (C4a, b)]. For IM, GV, and GM, this may also be seen from the governing equations for η (3.6), (3.14), and (3.20) which reduce directly to (2.23). In this limit, wall boundary conditions for the intermediate models will likewise reduce to (2.26). Note from (C13d) that the reduction of HP to QG for $\epsilon \to 0$ appear to depend on the requirement $F = O(1) > O(\epsilon)$. The behavior of HP in the limit $F \to 0$ with $h_B \neq 0$ is inaccurate as shown from the exact solutions in sections 6 and 7.

b. Linear ageostrophic coastally-trapped waves

As mentioned in section 1, the importance of linear ageostrophic coastally trapped wave motion to the observed behavior of continental shelf flow fields is well known. Consequently, the ability of intermediate models to represent these waves properly is of direct interest and is examined below.

The linear shallow-water equations for motion over O(1) topographic variations are

$$\epsilon F\eta_t + (Hu)_x + (Hv)_y = 0, \tag{4.1a}$$

$$\epsilon u_t - v = -\eta_x, \tag{4.1b}$$

$$\epsilon v_t + u = -\eta_y, \tag{4.1c}$$

where $H = 1 - h_B$. It follows from (4.1b, c) that

$$\mathcal{L}u = -\eta_y - \epsilon\eta_{xt}, \quad \mathcal{L}v = \eta_x - \epsilon\eta_{yt}, \tag{4.2a,b}$$

where

$$\mathcal{L} = 1 + \epsilon^2\partial^2/\partial t^2. \tag{4.2c}$$

Substituting (4.2a, b) in $\mathcal{L}$ (4.1a), we obtain a single equation for η:

$$[(H\eta_x)_x + (H\eta_y)_y - F\mathcal{L}\eta]_t = -\epsilon^{-1}J(\eta, h_B). \tag{4.3}$$

For definiteness, we assume that when solid boundaries are utilized in the following discussion, they exist at constant values of y, e.g., $y = y_0$, such that $v(y = y_0) = 0$ and $h_{Bx}(y = y_0) = 0$. In that case, (4.2b) implies a boundary condition for (4.3) of

$$\eta_x - \epsilon\eta_{yt} = 0, \quad \text{at} \quad y = y_0. \tag{4.4}$$

For all of the intermediate models, except for HP which is considered separately below, the following single governing equation for η may be found in the linear limit:

$$[(H\eta_x)_x + (H\eta_y)_y - F\eta]_t = -\epsilon^{-1}J(\eta, h_B), \tag{4.5}$$

with wall boundary condition given by (4.4). This result may be obtained from the linear limit of the equations in appendix C, which include $\nabla^2\psi = \nabla^2\eta$ and $\nabla^2\chi = -\nabla^2\psi_t$ or $\nabla^2\chi = -\nabla^2\eta_t$. We assume that wall boundary conditions (Part III) are such that these equations imply $\psi = \eta$ and $\chi = -\eta_t$. Consequently, (4.4) follows from (C1b). The corresponding QG linear equation is

$$[\nabla^2\eta_0 - F\eta_0]_t = -\epsilon^{-1}J(\eta_0, h_B), \tag{4.6}$$

with boundary condition (2.26).

We can see that the intermediate model equation (4.5) is the same as (4.3) with $\mathcal{L}$ approximated by 1, and that both (4.5) and (4.3) have the same boundary condition (4.4). In fact, (4.5) and (4.4) are the same equation and boundary condition that are derived in the standard linear low-frequency approximation for subinertial frequency motion, where it is assumed that

$$\epsilon^2 u_{tt} \ll u, \quad \epsilon^2 v_{tt} \ll v, \tag{4.7a,b}$$

and $\mathcal{L}$ is replaced by 1 in (4.2a, b). The intermediate models consequently represent linear ageostrophic coastally trapped waves with the same accuracy as the standard linear low-frequency approximation (4.7a, b). The QG approximation (4.6), on the other hand, drops all the H variability on the left hand side of (4.3) and replaces boundary condition (4.4) with (2.26).

As an example, we consider coastally trapped Kelvin waves for fluid in the region $y \geq 0$ with coast at $y_0 = 0$ and a flat bottom ($h_B \equiv 0$) in which case (4.3) from the linear SWE becomes

$$[\eta_{xx} + \eta_{yy} - F\mathcal{L}\eta]_t = 0. \tag{4.8}$$

Coastally-trapped wave motion of the form

$$\eta = C\exp(-i\omega t + ikx - ry), \tag{4.9}$$

satisfying (4.8) and (4.4), exists with

$$r = r_{SW} = F^{1/2}, \tag{4.10a}$$

$$\epsilon\omega = \epsilon\omega_{SW} = k/r_{SW}. \tag{4.10b}$$

For the intermediate models, with $h_B = 0$, (4.5) is

$$[\eta_{xx} + \eta_{yy} - F\eta]_t = 0. \tag{4.11}$$

A wave solution (4.9) satifies (4.11) and (4.4) with

$$r = r_I = (k^2 + F)^{1/2}, \tag{4.12a}$$

$$\epsilon\omega = \epsilon\omega_I = k/r_I. \tag{4.12b}$$

For $(\epsilon\omega_{SW})^2 \ll 1$, (4.12b) gives

$$\epsilon\omega_I = \epsilon\omega_{SW}\left[1 - \frac{1}{2}(\epsilon\omega_{SW})^2 + O(\epsilon^4\omega_{SW}^4)\right]. \tag{4.13}$$

Thus, the dispersion relation (4.12b) is a good approximation to (4.10b) for $(\epsilon\omega_{SW})^2 \ll 1$. The phase velocities $c_I = \omega_I/k = (\epsilon r_I)^{-1}$ and $c_{SW} = \omega_{SW}/k = (\epsilon F^{1/2})^{-1}$, so that $c_{SW} \geq c_I \geq 0$ and $(c_{SW} - c_I)$ increases as k increases. In the QG approximation with $h_B \equiv 0$, (4.6) reduces also to (4.11). The boundary condition (2.26), however, implies $C = 0$ for an as-

sumed solution (4.9) and thus filters out coastal Kelvin waves.

In the linear limit for Salmon's equations HP, (3.25) becomes

$$[(H\eta_x)_x + (H\eta_y)_y - F\eta]_t = \epsilon^{-1}J(h_B, \mathcal{B}'_{HP}), \quad (4.14a)$$

where

$$\mathcal{B}'_{HP} = \eta + (\epsilon/F)H\zeta_A - (\epsilon/F)(-u_A h_{By} + v_A h_{Bx}). \quad (4.14b)$$

The diagnostic equations (A13) reduce to (A20) and the momentum equation (3.23a) is

$$\epsilon u_{Gt} - v = -\mathcal{B}'_{HPx}. \quad (4.15)$$

For the flat bottom case ($h_B \equiv 0$), (4.14a) reduces to (4.11) and (A20a, b) become

$$\nabla^2 u_A - Fu_A = 0, \quad \nabla^2 v_A - Fv_A = 0. \quad (4.16a,b)$$

The boundary condition (A17a), $u_A(y = 0) = 0$, and (4.16a) imply

$$u_A \equiv 0. \quad (4.17)$$

The boundary condition $v\,(y = 0) = 0$ gives

$$\epsilon v_A = -v_G = -\eta_x, \quad \text{at} \quad y = 0, \quad (4.18)$$

and implies from (4.15),

$$-\epsilon\eta_{yt} = -\eta_x + F^{-1}\eta_{xxx}, \quad \text{at} \quad y = 0, \quad (4.19)$$

where (4.17) and (4.18) have been used to substitute $\epsilon\zeta_{Ax}(y = 0) = -\eta_{xxx}$ in (4.15). A coastally trapped Kelvin wave solution may be found from (4.11) with boundary condition (4.19) and is given by (4.9) with (4.12a) and

$$\epsilon\omega = \epsilon\omega_{HP} = kr_I/F. \quad (4.20)$$

For $(\epsilon\omega_{SW})^2 \ll 1$, (4.20) gives

$$\epsilon\omega_{HP} = \epsilon\omega_{SW}\left[1 + \frac{1}{2}(\epsilon\omega_{SW})^2 + O(\epsilon^4\omega_{SW}^4)\right], \quad (4.21)$$

so that the dispersion relation (4.20) is also a good approximation to (4.10b) for $(\epsilon\omega_{SW})^2 \ll 1$ and $k = O(1)$. In this case, however, the phase velocity $c_{HP} \geqslant c_{SW} \geqslant 0$ and $(c_{HP} - c_{SW})$ increases as k increases so that the large k waves propagate with phase velocity that is greater than the exact phase velocity for the SWE. This is the opposite to the behavior for c_I as k increases and may be expected to cause restrictions on the time-step in the application of explicit finite difference numerical methods.

For a second example, we consider free waves in an infinite constant-width channel $0 \leqslant y \leqslant 1$ with across-channel topographic variations

$$H = \exp(-sy), \quad (4.22)$$

in the limiting case $F \to 0$. Assuming

$$\eta = g(y)\exp(-i\omega t + ikx), \quad (4.23)$$

we find for both the SWE (4.3) and the intermediate models (4.5) (except HP) that g satisfies

$$g_{yy} - sg_y + (-k^2 - sb^{-1})g = 0, \quad (4.24)$$

with boundary conditions from (4.4) of

$$g + bg_y = 0, \quad \text{at} \quad y = 0, 1, \quad (4.25)$$

where

$$b = \epsilon\omega/k. \quad (4.26)$$

The solutions are

$$g = C\exp\left(\frac{1}{2}ys\right)\left[\sin n\pi y - n\pi b \times \left(1 + \frac{1}{2}bs\right)^{-1}\cos n\pi y\right], \quad (4.27a)$$

where $n = 1, 2, \cdots$, and

$$b = -s\left[k^2 + (n\pi)^2 + \frac{1}{4}s^2\right]^{-1}, \quad (4.27b)$$

and they represent subinertial frequency topographic Rossby waves. For $s = O(1)$, $n\pi = O(1)$, $k \leqslant O(1)$, these waves are ageostrophic, i.e., $b = O(1)$ so that bg_y is the same magnitude as g in (4.2b). For $s = O(\epsilon)$ and $H = 1 - sy + O(\epsilon^2)$, (4.27a, b) reduce with relative error $O(\epsilon)$ to the quasi-geostrophic solutions,

$$g = C\sin n\pi y, \quad (4.28a)$$

$$b = -s[k^2 + (n\pi)^2]^{-1}, \quad (4.28b)$$

for constant bottom slope. Consequently, in this example with $F \to 0$, the intermediate model solutions (except HP) represent the exact SWE ageostrophic waves when $s = O(1)$ and they reduce to the QG results when $s = O(\epsilon)$.

5. Exact solutions of the shallow-water equations

Exact nonlinear analytical solutions of the SWE for steady flow in an elliptic paraboloid have been found by Ball (1965) and for unsteady elliptical vortices by Cushman-Roisin et al. (1985) (see also, Cushman-Roisin 1987; Young 1987). These flows are characterized by spatially constant vorticity and zero divergence. The analysis procedure for both proceeds similarly. The time-dependent solutions of Cushman-Roisin et al. (1985) correspond to steadily rotating elliptic eddies and have been named Rodons. Unsteady motion with dynamics similar to the Rodon is found here to exist in a circular paraboloid and to reduce to the Rodon solution as the bottom topographic variations vanish. Corresponding exact analytical solutions to the intermediate models may also be found for the same situations. A comparison of these with the exact results from the SWE thus allows a direct assessment of the relative accuracy of the intermediate models in these particular cases. The relevant exact solutions for

the SWE are obtained here and those for the intermediate models in section 6. The results are discussed and compared in section 7.

Following Ball (1965), we consider motion in an elliptic paraboloid with bottom topography

$$h_B = \tfrac{1}{2}\alpha x^2 + \tfrac{1}{2}\beta y^2, \quad \alpha, \beta \geq 0. \quad (5.1a,b)$$

Solutions are sought in the form

$$u = U_1 x + U_2 y, \quad v = V_1 x + V_2 y, \quad (5.2a,b)$$

$$\eta = \eta_0 + \tfrac{1}{2}Ax^2 + Bxy + \tfrac{1}{2}Cy^2, \quad (5.2c)$$

where the coefficients U_1, etc. are functions of time. Substitution of (5.1) and (5.2) in (2.1) results in eight nonlinear ordinary differential equations for the eight coefficients. It is more convenient to work with the following variables (Ball 1965):

$$\zeta = v_x - u_y = V_1 - U_2, \quad (5.3a)$$

$$D = u_x + v_y = U_1 + V_2, \quad (5.3b)$$

$$M = v_x + u_y = V_1 + U_2, \quad (5.3c)$$

$$L = u_x - v_y = U_1 - V_2, \quad (5.3d)$$

$$R = \eta_{xx} + \eta_{yy} = A + C, \quad (5.3e)$$

$$S = 2\eta_{xy} = 2B, \quad (5.3f)$$

$$Q = \eta_{xx} - \eta_{yy} = A - C. \quad (5.3g)$$

The resulting equations for the variables defined in (5.3) are

$$\epsilon\zeta_t + (\epsilon\zeta + 1)D = 0, \quad (5.4a)$$

$$\epsilon D_t + \tfrac{1}{2}\epsilon(D^2 + L^2 + M^2 - \zeta^2) - \zeta = -R, \quad (5.4b)$$

$$\epsilon M_t + \epsilon MD + L = -S, \quad (5.4c)$$

$$\epsilon L_t + \epsilon LD - M = -Q, \quad (5.4d)$$

$$R_t + SM + 2D(R - \hat{\theta}) + L(Q - \hat{\phi}) = 0, \quad (5.4e)$$

$$Q_t + S\zeta + 2D(Q - \hat{\phi}) + L(R - \hat{\theta}) = 0, \quad (5.4f)$$

$$S_t + 2SD + M(R - \hat{\theta}) - \zeta(Q - \hat{\phi}) = 0, \quad (5.4g)$$

$$\epsilon F\eta_{0t} + (\epsilon F\eta_0 + 1)D = 0, \quad (5.4h)$$

where

$$\hat{\theta} = \theta/\epsilon F, \quad \hat{\phi} = \phi/\epsilon F, \quad (5.5a,b)$$

$$\theta = \alpha + \beta, \quad \phi = \alpha - \beta. \quad (5.5c,d)$$

Also, for use below we define,

$$\tilde{\theta} = \theta/F, \quad \tilde{\phi} = \phi/F. \quad (5.6a,b)$$

Steady solutions of (5.4) for $\tilde{\phi} \neq 0$ are given by

$$D = 0, \quad L = -S = 0, \quad M = Q, \quad (5.7a,b,c)$$

$$R = \zeta + \tfrac{1}{2}\epsilon(\zeta^2 - Q^2), \quad (5.7d)$$

$$Q = \frac{\zeta\tilde{\phi}}{[\tilde{\theta} - \epsilon(R - \zeta)]}. \quad (5.7e)$$

The above solutions are valid also in the limit $\tilde{\phi} \to 0$, but for $\tilde{\phi} = 0$ additional steady solutions with $L \neq 0$ and $S \neq 0$ are possible. These turn up as zero frequency solutions in the unsteady case considered below. This same situation also occurs with the intermediate models in section 7. The substitution of (5.7e) in (5.7d) gives the following cubic equation for

$$T = \epsilon(R - \zeta), \quad (5.8a)$$

$$T^3 - \left(2\tilde{\theta} + \tfrac{1}{2}\epsilon^2\zeta^2\right)T^2 + (\tilde{\theta}^2 + \tilde{\theta}\epsilon^2\zeta^2)T - \tfrac{1}{2}\epsilon^2\zeta^2(\tilde{\theta}^2 - \tilde{\phi}^2) = 0. \quad (5.8b)$$

With given topography and parameter F, which appears as the combinations $\tilde{\theta}$ and $\tilde{\phi}$, and a specified value of the vorticity $\epsilon\zeta$, the possible steady values of R are given by the solutions to (5.8). Q may then be found from (5.7d). The results are discussed in section 7. To insure physically realizable solutions, we require $\epsilon FA < \alpha$ and $\epsilon FC < \beta$ or

$$\tfrac{1}{2}(R + Q) < \hat{\alpha}, \quad \tfrac{1}{2}(R - Q) < \hat{\beta}. \quad (5.9a,b)$$

For the unsteady case, we consider the class of motions (Cushman-Roisin et al. 1985; Cushman-Roisin 1987) governed by (5.4) for which

$$D = 0. \quad (5.10)$$

With (5.10), (5.4) reduce to

$$\zeta_t = 0, \quad (5.11a)$$

$$\tfrac{1}{2}\epsilon(L^2 + M^2 - \zeta^2) - \zeta = -R, \quad (5.11b)$$

$$\epsilon M_t + L = -S, \quad (5.11c)$$

$$\epsilon L_t - M = -Q, \quad (5.11d)$$

$$R_t + SM + L(Q - \hat{\phi}) = 0, \quad (5.11e)$$

$$Q_t + S\zeta + L(R - \hat{\theta}) = 0, \quad (5.11f)$$

$$S_t + M(R - \hat{\theta}) - \zeta(Q - \hat{\phi}) = 0, \quad (5.11g)$$

$$\epsilon F\eta_{0t} = 0. \quad (5.11h)$$

Substituting (5.11a, c, d, e) in the time derivative of (5.11b), we obtain

$$LQ + MS - \tfrac{1}{2}L\hat{\phi} = 0. \quad (5.12)$$

Note that (5.11b) is analogous to an equation of balance (3.30) while (5.12) is the corresponding omega equation analogous to (3.31). The substitution of (5.12) in (5.11e) gives

$$R_t - \tfrac{1}{2} L\hat{\phi} = 0, \tag{5.13}$$

which may be used in place of (5.11e).

Analytical solutions in terms of simple functions may be found when the topography is a circular paraboloid,

$$\hat{\phi} = \hat{\alpha} - \hat{\beta} = 0. \tag{5.14}$$

In this case, (5.12), (5.13) and (5.11g) reduce to

$$LQ + MS = 0, \tag{5.15a}$$

$$R_t = 0, \tag{5.15b}$$

$$S_t + M(R - \hat{\theta}) - \zeta Q = 0. \tag{5.15c}$$

Solutions to (5.11a, b, c, d) and (5.15a, b, c) may be found (Cushman-Roisin et al. 1985) in the form,

$$\zeta = \zeta_0, \quad R = R_0, \tag{5.16a,b}$$

$$(L, S) = (L_0, Q_0)\sin(\omega t + \Theta_0), \tag{5.16c,d}$$

$$(M, Q) = (-L_0, Q_0)\cos(\omega t + \Theta_0), \tag{5.16e,f}$$

if ω satisfies

$$\epsilon\omega^2 + (1 - \epsilon\zeta)\omega + (R - \zeta - \hat{\theta}) = 0, \tag{5.17}$$

and

$$R = R_0 = \zeta + \frac{\epsilon}{2}(\zeta^2 - L_0^2), \tag{5.18a}$$

$$Q_0 = -L_0(1 + \epsilon\omega). \tag{5.18b}$$

For $\tilde{\theta} = 0$, the two roots to (5.17) give one subinertial and one superinertial frequency. The subinertial frequency of interest here is given by

$$\epsilon\omega = -\tfrac{1}{2}(1 - \epsilon\zeta) + \tfrac{1}{2}[(1 + \epsilon\zeta)^2 - 4\epsilon R + 4\tilde{\theta}]^{1/2}, \tag{5.19}$$

where we assume $\tilde{\theta} < 2$ is small enough that $|\epsilon\omega| < 1$.

When the topography vanishes, $\tilde{\theta} = 0$, these solutions reduce to the steadily rotating elliptical eddy Rodon of Cushman-Roisin et al. (1985). For $\tilde{\theta} \neq 0$, the dynamics remain similar, but the frequency (5.19) is altered by the presence of the topography. The solutions are determined here by the assumption that $\epsilon\zeta_0$ and ϵL_0 (and an initial value of the phase Θ_0) are specified. This specification is different than that used by Cushman-Roisin et al. (1985) where, for convenience in relating the results to satellite observations of eddy sizes and ellipticities, it is assumed that R_0 and Q_0 are known. For our purposes, however, it seems sensible to retain consistency with the steady solutions, where the specification of $\epsilon\zeta_0$ was natural, and to assume properties of the velocity field $\epsilon\zeta_0$ and ϵL_0 are given.

The frequency (5.19) and R (5.18a) may be written as

$$\epsilon\omega = -\tfrac{1}{2}(1 - \epsilon\zeta) + \tfrac{1}{2}[2(1 + \epsilon^2 L_0^2 + 2\tilde{\theta}) - (1 + \epsilon\zeta)^2]^{1/2}, \tag{5.20}$$

$$2\epsilon R = (1 + \epsilon\zeta)^2 - (1 + \epsilon^2 L_0^2), \tag{5.21}$$

and it follows from (5.20), (5.21) and (5.18b) that

$$4\epsilon^2[(R - \hat{\theta})^2 - Q_0^2] = (1 + 2\tilde{\theta})^2 - \{(1 + \epsilon\zeta)[2(1 + \epsilon^2 L_0^2 + 2\tilde{\theta}) - (1 + \epsilon\zeta)^2]^{1/2} + \epsilon^2 L_0^2\}^2. \tag{5.22}$$

Real values of $\epsilon\omega$ are found from (5.20) provided

$$2(1 + \epsilon^2 L_0^2 + 2\tilde{\theta}) \geq (1 + \epsilon\zeta)^2. \tag{5.23}$$

For physical realizability it is required that

$$R < \hat{\theta}, \quad Q_0^2 < (R - \hat{\theta})^2. \tag{5.24a,b}$$

From (5.21), (5.24a) requires

$$(1 + \epsilon^2 L_0^2 + 2\tilde{\theta}) > (1 + \epsilon\zeta^2), \tag{5.25}$$

which, if satisfied, implies that (5.23) is satisfied. Condition (5.24b) may be found in terms of ζ and L_0 from (5.22) and reduces to

$$(1 + \epsilon^2 L_0^2 + 2\tilde{\theta}) - 2\epsilon|L_0|(1 + 2\tilde{\theta})^{1/2} > (1 + \epsilon\zeta)^2, \tag{5.26a}$$

or

$$[(1 + 2\tilde{\theta})^{1/2} - \epsilon|L_0|]^2 > (1 + \epsilon\zeta)^2. \tag{5.26b}$$

It also follows from (5.22) that

$$4\epsilon^2[(R - \hat{\theta})^2 - Q_0^2] \leq (1 + 2\tilde{\theta})^2, \tag{5.27}$$

which gives a minimum value of the eddy mean radius. When $\tilde{\theta} = 0$, (5.24a, b) and (5.27) reduce to the proper existence conditions for the Rodon (Cushman-Roisin et al. 1985).

6. Exact solutions of the intermediate models

Corresponding exact analytical results for the intermediate models may be found for the topography (5.1) by seeking solutions of the form (5.2). We present the resulting ordinary differential equations and obtain the relevant solutions in terms of the variables (5.3) in this section. For the intermediate models that utilize the full continuity equation (2.1a), (5.4e, f, g, h) remain unchanged and we will assume that they apply here unless specifically noted. The intermediate models involve different approximations to the momentum equations and thus (5.4a, b, c, d) are replaced with the equations given below.

a. Intermediate model—IM

$$\epsilon R_t + D = 0, \tag{6.1a}$$

$$\tfrac{1}{2}\epsilon(Q^2 + S^2 - R^2) - \zeta = -R, \tag{6.1b}$$

$$\epsilon Q_t + L = -S, \tag{6.1c}$$

$$\epsilon S_t + M = Q. \tag{6.1d}$$

The steady solutions are (5.7a, b, c),

$$R = \zeta + \tfrac{1}{2}\epsilon(R^2 - Q^2), \tag{6.2}$$

and (5.7e). A quartic equation for $T = \epsilon(R - \zeta)$ results from the substitution of (5.7e) in (6.2).

The unsteady solutions with $D = 0$, $\tilde{\phi} = 0$, and with the variables written in the form (5.16) are

$$R = \zeta + \tfrac{1}{2}\epsilon(R^2 - Q_0^2), \tag{6.3a}$$

$$Q_0 = -\frac{(1 - \epsilon R + \tilde{\theta})}{(1 - \epsilon\zeta)} L_0, \tag{6.3b}$$

$$\epsilon\omega = \frac{\tilde{\theta} + \epsilon(\zeta - R)}{(1 - \epsilon R + \tilde{\theta})}. \tag{6.3c}$$

A quadratic equation for T follows from (6.3a, b).

b. Geostrophic vorticity—GV

$$\epsilon R_t + (\epsilon R + 1)D = 0, \tag{6.4a}$$

$$\tfrac{1}{2}\epsilon(Q^2 + S^2 + R^2 - 2R\zeta) - \zeta = -R, \tag{6.4b}$$

$$\epsilon Q_t + \epsilon SR + (\epsilon R + 1)L = -S, \tag{6.4c}$$

$$\epsilon S_t - \epsilon QR + (\epsilon R + 1)M = Q. \tag{6.4d}$$

The steady solutions are (5.7a, b, c, e) and

$$R = \zeta + \tfrac{1}{2}\epsilon(2R\zeta - R^2 - Q^2). \tag{6.5}$$

A quartic equation for T follows from (5.7e) and (6.5).

The unsteady solutions with $D = 0$, $\tilde{\phi} = 0$ are

$$R = \zeta + \tfrac{1}{2}\epsilon(2R\zeta - R^2 - Q_0^2), \tag{6.6a}$$

$$Q_0 = -\frac{(1 + \tilde{\theta})L_0}{[1 + \epsilon(R - \zeta)]}, \tag{6.6b}$$

$$\epsilon\omega = \frac{(1 + \epsilon R)[\tilde{\theta} + \epsilon(\zeta - R)]}{(1 + \tilde{\theta})}. \tag{6.6c}$$

A quartic equation for T results from (6.6a, b).

c. Geostrophic momentum—GM

$$\epsilon R_t + \tfrac{1}{2}\epsilon(SM + DR + LQ) + D = 0, \tag{6.7a}$$

$$\tfrac{1}{2}\epsilon(MQ - LS - \zeta R) - \zeta = -R, \tag{6.7b}$$

$$\epsilon Q_t + \tfrac{1}{2}\epsilon(S\zeta + DQ + LR) + L = -S, \tag{6.7c}$$

$$\epsilon S_t + \tfrac{1}{2}\epsilon(MR - \zeta Q) + M = Q. \tag{6.7d}$$

The steady solutions are (5.7a) and

$$\left(1 + \tfrac{1}{2}\epsilon R\right)M = \left(1 + \tfrac{1}{2}\epsilon\zeta\right)Q, \tag{6.8a}$$

$$R = \zeta + \tfrac{1}{2}\epsilon(2R\zeta - R^2 - Q^2) + \tfrac{1}{4}\epsilon^2\zeta(R^2 - Q^2), \tag{6.8b}$$

$$Q = \frac{\zeta\tilde{\phi}\left(1 + \tfrac{1}{2}\epsilon R\right)}{\left[\tilde{\theta}\left(1 + \tfrac{1}{2}\epsilon\zeta\right) - \epsilon(R - \zeta)\right]}. \tag{6.8c}$$

A quartic equation for T follows from (6.8b, c).

The unsteady solutions with $D = 0$, $\tilde{\phi} = 0$ are

$$R = \zeta + \frac{1}{2}\epsilon\left[\zeta R - L_0^2 \frac{\left(1 + \tilde{\theta} - \tfrac{1}{2}\epsilon R\right)}{\left(1 - \tfrac{1}{2}\epsilon\zeta\right)}\right], \tag{6.9a}$$

$$Q_0 = -\frac{\left(1 + \tilde{\theta} - \tfrac{1}{2}\epsilon R\right)}{\left(1 - \tfrac{1}{2}\epsilon\zeta\right)} L_0, \tag{6.9b}$$

$$\epsilon\omega = \frac{\left[\tilde{\theta}\left(1 + \tfrac{1}{2}\epsilon\zeta\right) + \epsilon(\zeta - R)\right]}{\left(1 + \tilde{\theta} - \tfrac{1}{2}\epsilon R\right)}, \tag{6.9c}$$

where (6.9a) is a linear equation for T.

d. Salmon's equations—HP

$$\epsilon R_t + (\epsilon R + 1)D = 0, \tag{6.10a}$$

$$\tfrac{1}{2}\epsilon[2(QM - SL + R\zeta) - Q^2 - S^2 - 3R^2] - \zeta = -R - 2(R - \zeta)\tilde{\theta} + (M - Q)\tilde{\phi}, \tag{6.10b}$$

$$\epsilon Q_t + \tfrac{1}{2}\epsilon[-S(R - \zeta) + 2QD] + L = -S + D\tilde{\phi} - (L + S)\tilde{\theta}, \tag{6.10c}$$

$$\epsilon S_t + \tfrac{1}{2}\epsilon[Q(R - \zeta) + 2SD] = Q + 2(R - \zeta)\tilde{\phi} - (M - Q)\tilde{\theta}. \tag{6.10d}$$

The steady solutions are (5.7a) and

$$R = \zeta + \frac{1}{2}\frac{\epsilon(R^2 - Q^2)(1 + \tilde{\theta})}{[(1 - \epsilon R + 2\tilde{\theta})(1 + \tilde{\theta}) - 2(\tilde{\phi} - \epsilon Q)^2]}, \tag{6.11a}$$

$$Q = \tilde{\phi}\,\frac{[\zeta(1+\tilde{\theta}) - 2(R-\zeta)(\tilde{\theta} - \epsilon R)]}{[\tilde{\theta} + \tilde{\theta}^2 - \epsilon(R-\zeta)(1 + 3\tilde{\theta} - 2\epsilon R)]}. \tag{6.11b}$$

A sixth-order polynomial for T follows from (6.11a, b).

The unsteady solutions ($D = 0$, $\tilde{\phi} = 0$) are

$$R = \zeta + \frac{1}{2}\epsilon\,\frac{(Q_0^2 + R^2 - 2|Q_0||L_0|)}{(1 - \epsilon R + 2\tilde{\theta})}, \tag{6.12a}$$

$$Q_0 = -\frac{(1 - \epsilon R + 2\tilde{\theta})}{[1 - 2\epsilon(R-\zeta) - \epsilon\zeta + \tilde{\theta}]}\,L_0, \tag{6.12b}$$

$$\epsilon\omega = \frac{[\tilde{\theta} + \tilde{\theta}^2 - \epsilon(R-\zeta)(1 + 3\tilde{\theta} - 2\epsilon R)]}{(1 - \epsilon R + 2\tilde{\theta})}. \tag{6.12c}$$

The combination of (6.12a, b) results in a quartic equation for T.

e. Balance equations—BE, HBE, BEM, NBE

The intermediate models BE, HBE, BEM, and NBE involve the use of functions ψ and χ to represent the velocity field. A general representation of both ψ and χ in a form similar to that for η in (5.2c) would require a total of six coefficients for the x^2, y^2, and xy terms. The representation of the velocity field (5.2a, b) for the exact solution of the SWE, however, involves only four coefficients U_1, U_2, V_1, V_2 (or alternately ζ, D, M, L). The two extra coefficients in ψ and χ correspond to the case $\epsilon\chi_x = \psi_y$, $\epsilon\chi_y = -\psi_x$ so $u = v = 0$, but ψ, $\chi \neq 0$. We proceed by assuming

$$\psi = \tfrac{1}{4}(M+\zeta)x^2 - \tfrac{1}{2}Lxy - \tfrac{1}{4}(M-\zeta)y^2, \tag{6.13a}$$

$$\epsilon\chi = \tfrac{1}{4}D(x^2 + y^2), \tag{6.13b}$$

so that

$$u = -\psi_y + \epsilon\chi_x = \tfrac{1}{2}(D+L)x + \tfrac{1}{2}(M-\zeta)y, \tag{6.14a}$$

$$v = \psi_x + \epsilon\chi_y = \tfrac{1}{2}(M+\zeta)x + \tfrac{1}{2}(D-L)y, \tag{6.14b}$$

consistent with (5.2a, b) and (5.3a, b, c, d).

For HBE, the substitution of (6.13) and (6.14) in (3.40) results in

$$\epsilon\zeta_t + D = 0, \tag{6.15a}$$

$$\tfrac{1}{2}\epsilon(L^2 + M^2 - \zeta^2) - \zeta = -R, \tag{6.15b}$$

$$\epsilon M_t + L = -S, \tag{6.15c}$$

$$\epsilon L_t - M = -Q. \tag{6.15d}$$

For BEM, the use of (6.13) and (6.14) in (3.44) gives the same equations (6.15b, c, d) with (6.15a) replaced by

$$\epsilon\zeta_t + (1 + \epsilon\zeta)D = 0. \tag{6.16}$$

Steady solutions of (6.15) and (6.16) require $D = 0$ while the unsteady solutions are obtained under the assumption $D = 0$. In that case, (6.15) and (6.16) reduce to equations that are identical to those obtained from (5.11a, b, c, d) for the SWE. Consequently, for the special problems considered here, HBE and BEM will give results identical to those from the SWE. A similar result holds with $D = 0$ for NBE also. For BE, with (6.13) and (6.14) the vorticity equation and the balance equation do not provide sufficient information to determine the four coefficients D, ζ, L, M and momentum equations must be utilized. With $D = 0$, the equivalent momentum equations of BE are the same as (3.44) for BEM and we conclude that BE also will give solutions that are identical to those from the SWE.

f. Linear balance equations—LBE, LQBE

With our interpretation of LBE (section 3f), the momentum equations are the same as IM (6.1). The velocity components for the continuity equation (3.35), found using (5.2a) and (6.13b), are

$$u_G + \epsilon\chi_x = -\left(B - \tfrac{1}{2}D\right)x - Cy, \tag{6.17a}$$

$$v_G + \epsilon\chi_y = Ax + \left(B + \tfrac{1}{2}D\right)y. \tag{6.17b}$$

As a result, (5.4e, f, g) from the continuity equation are replaced in LBE by

$$R_t + S\hat{\phi} + 2D(R - \hat{\theta}) = 0, \tag{6.18a}$$

$$Q_t + S\hat{\theta} + 2D(Q - \hat{\phi}) = 0, \tag{6.18b}$$

$$S_t + R\hat{\phi} - Q\hat{\theta} + 2SD = 0. \tag{6.18c}$$

Steady solutions are (5.7a, b, c, e), (6.2) and

$$Q = \tilde{\phi}R/\tilde{\theta}. \tag{6.19}$$

A quadratic equation for T follows from substituting (6.19) in (6.2).

The unsteady solutions ($D = 0$, $\hat{\phi} = 0$) are (6.3a), which is a quadratic for T, and

$$Q_0 = -L_0/(1 - \tilde{\theta}), \tag{6.20a}$$

$$\epsilon\omega = \tilde{\theta}. \tag{6.20b}$$

For LQBE, with $D = 0$, and hence $\chi = 0$ (6.13b), the momentum equations (3.38) reduce to those of IM (3.4). The continuity equation is the same as LBE (3.35). Consequently, the equations and results here for LQBE are the same as for LBE.

g. Quasi-geostrophic—QG

Corresponding solutions may be obtained for QG from (2.14), (2.16), and (2.19) if we assume that u, v, and η in (5.2) represent

$$u = u_0 + \epsilon u_1, \quad v = v_0 + \epsilon v_1, \tag{6.21a,b}$$

$$\eta = \eta_0 + \epsilon\eta_1, \tag{6.21c}$$

add (2.14a) to (2.16b) and (2.14b) to (2.16a) and then replace η_0 in (2.14) with η. This is equivalent to the assumptions utilized in deriving QG from (3.4) and (3.8). The resulting momentum equations are the same as IM (3.4) and (6.1). The continuity equations, replacing (5.4e, f, g), are

$$R_t + S\hat{\phi} = 0, \tag{6.22a}$$

$$Q_t + S\hat{\theta} = 0, \tag{6.22b}$$

$$S_t + R\hat{\phi} - Q\hat{\theta} = 0. \tag{6.22c}$$

The steady and unsteady solutions are the same as for LBE [(5.7a, b, c, e), (6.2), (6.19)] and [(6.3a), (6.20a, b)].

h. Modified slow equations—MSE

With $D = D' = 0$, the MSE momentum (3.69a, b) and continuity (3.65) equations reduce to those of BEM. Thus for these problems, MSE will give the same solutions as the SWE, similar to BEM, BE, HBE, and NBE.

7. Comparison of exact solutions

We consider first the steady flow in an elliptic paraboloid for $0 \leqslant \epsilon < 1$ with either positive or negative vorticity ($\zeta = \pm 1$) and with variable values of the bottom topographic parameters and F, such that $0 \leqslant \tilde{\theta} < \infty$ and $0 \leqslant \tilde{\phi}/\tilde{\theta} \leqslant 1$. For the SWE, T is obtained from the numerical solution of the cubic equation (5.8b) to give $(R - \zeta)$ and Q is then found from (5.7e). Over much of the above defined parameter space, there is only one real root of (5.8b) that corresponds to a physically realizable solution such that (5.9) is satisfied. (The stability of the solutions is not considered here). An analysis of the coefficients in (5.8) shows that three real roots exist for values of $\tilde{\theta}$ and $\tilde{\phi}$ that satisfy

$$0 \geqslant \tilde{\phi}^2\left[\tilde{\phi}^2 - \frac{8}{27\epsilon^2}\left(\frac{1}{2}\epsilon^2 - \tilde{\theta}\right)^3\right]. \tag{7.1}$$

Asymptotic results verified by numerical calculations show that these correspond to three physically realizable solutions satisfying (5.9) when $\zeta < 0$. For the intermediate models, T is found from the numerical solution of the relevant polynominal equation.

It is useful to start with $\tilde{\phi} = 0$ where the geometry is that of a circular paraboloid and the flow corresponds to a circular vortex (Hoskins 1975; McWilliams and Gent 1980). For the SWE and all of the approximate models except HP the effects of geometry drop out when $\tilde{\phi} = 0$ and, as expected, the solutions become independent of the value of $\tilde{\theta}$. Curiously, that does not happen for HP where, for $\tilde{\phi} = 0$, (6.11a) reduces to

$$R = \zeta + \frac{1}{2}\epsilon\frac{R^2}{(1 - \epsilon R + 2\tilde{\theta})}, \tag{7.2}$$

and an erroneous dependence on $\tilde{\theta}$ is retained.

The solutions for $(R - \zeta)$ from the SWE, from QG, and from the intermediate models IM, GV, GM, and HP for the circular vortex $\tilde{\phi} = 0$ are shown in Fig. 1. For these solutions we set $\tilde{\theta} = 0$ and ignore the physical realizability constraint (5.9). Note that the method of presenting the results here, with $\epsilon\zeta$ assumed known, differs from those used in the previous papers. Also, recall that for all of the comparisons in this section, BE, HBE, BEM, NBE, and MSE give the same solutions as the SWE and that LBE and LQBE give the same results as QG.

We see from Fig. 1 that for the circular vortex GV generally produces the most accurate approximate solution over a large range of ϵ. The accuracy is best in all models when ϵ is small. HP does relatively poorly, producing a less accurate solution than QG and IM which give the same result in this case. The error of GM lies between that of GV and QG.

Values of $(R - \zeta)$ and Q for the steady flow in an elliptic paraboloid with $\tilde{\phi}/\tilde{\theta} = 0.5$ and $\tilde{\theta} = 1.0$ are shown in Fig. 2. The curves are terminated at values of ϵ for which (5.9a, b) cease to be satisfied when $\zeta = +1$. GV gives the most accurate approximation for both R and Q. IM and QG are the most inaccurate for $\zeta = +1$ while HP is poor for $\zeta = -1$. QG produces the largest errors in Q for ζ positive or negative.

The effect of an increased value of $\tilde{\theta}$ in the steady flow in an elliptic paraboloid is shown in Fig. 3 where the parameters are ($\tilde{\theta} = 2{,}000$, $\tilde{\phi}/\tilde{\theta} = 0.5$). This corresponds, for example, to increasing the magnitude of the Rossby radius with fixed topography. Again, GV gives the most accurate approximation. In HP, the suppression of variability of $(R - \zeta)$ with ϵ for large $\tilde{\theta}$, similar to that indicated by (7.2) for the flow in a

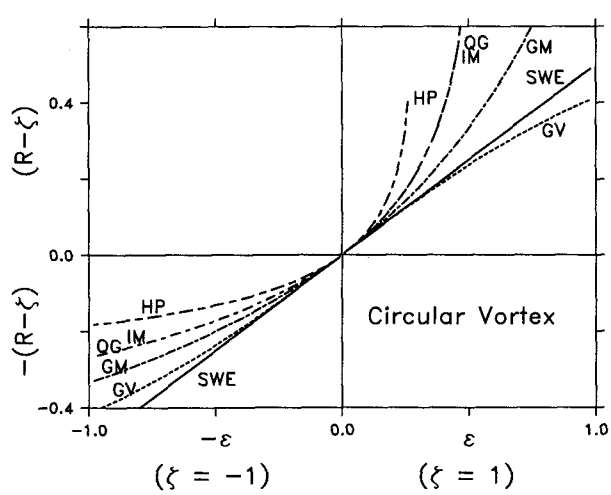

FIG. 1. Exact solutions for the steady circular vortex as a function of $0 \leqslant \epsilon < 1$ for $\zeta = \pm 1$. For convenience, we plot $(R - \zeta)$ vs ϵ for $\zeta = +1$ and $-(R - \zeta)$ vs $-\epsilon$ for $\zeta = -1$, as indicated. These solutions are obtained from those in a circular paraboloid $\tilde{\phi} = 0$ with $\tilde{\theta} = 0$ and the physical realizability constraint (5.9) ignored.

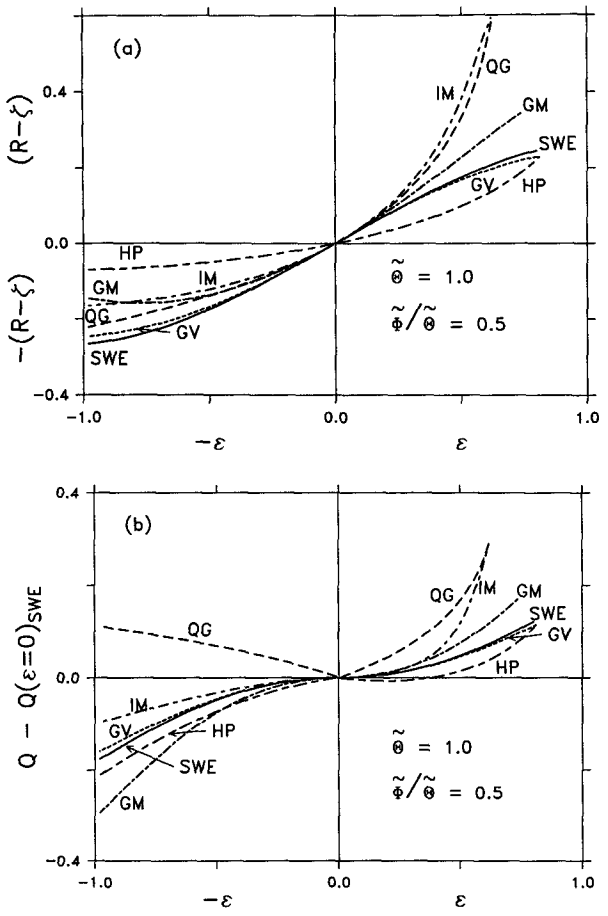

FIG. 2. Exact solutions for the steady flow in an elliptic paraboloid with $\tilde{\theta} = 1$ and $\tilde{\phi}/\tilde{\theta} = 0.5$ as a function of $0 \leq \epsilon < 1$ for $\zeta = \pm 1$; (a) $(R - \zeta)$ vs ϵ for $\zeta = +1$ and $-(R - \zeta)$ vs $-\epsilon$ for $\zeta = -1$; (b) $Q - Q(\epsilon = 0)_{SWE}$ vs ϵ for $\zeta = +1$ and vs $-\epsilon$ for $\zeta = -1$, where $Q(\epsilon = 0)_{SWE} = \zeta\tilde{\phi}/\tilde{\theta}$. The solutions for $\zeta = +1$ are not plotted at values of ϵ for which the physical realizability constraint (5.9) is not satisfied.

circular paraboloid, is evident here. IM gives an inaccurate approximation to R, with errors greater than QG, while QG again has the largest errors in Q. GM also gives an inaccurate result for Q. GM produces errors in R that are qualitatively similar to those it has in the circular vortex (Fig. 1) and thus again lies overall in accuracy between GV and QG.

The results for a set of parameter values when three steady solutions of the SWE are possible (7.1) are illustrated in Fig. 4 ($\zeta = -1$, $\tilde{\theta} = 0.02$, $\tilde{\phi}/\tilde{\theta} = 0.5$). This behavior forms an interesting comparison since SWE solutions for T are found from a cubic, whereas those for IM, GV, GM, and HP are found from higher order polynomials. QG is governed by a quadratic and only has one relevant solution. For $\epsilon \gtrsim 0.4$, the largest root for R ($R \approx \zeta + \frac{1}{2}\epsilon\zeta^2$) goes with the middle solution for Q ($Q \approx 0$) and corresponds to the circular vortex that exists in the limit $\tilde{\theta} \to 0$ and that arises for small values of $\tilde{\theta}$ that satisfy (7.1). The smallest solution for R ($R \approx -1$) goes with the most negative Q ($Q \approx -1$ for $\epsilon \gtrsim 0.3$) and corresponds to a long elliptical eddy with major axis in the y direction such that in the limit $\tilde{\theta} \to 0$, $A \sim -1$ and $C \sim 0$. This root corresponds to the small $\tilde{\theta}$ limit of the single physically relevant solution over most of the ($\tilde{\theta}$, ϵ, $\tilde{\phi}/\tilde{\theta} = 0.5$) parameter space. The remaining solution for R when $\epsilon \gtrsim 0.4$ goes with the solution $Q \approx 1$ and corresponds to a long elliptical eddy with major axis in the x direction such that for $\tilde{\theta} \to 0$, $A \sim 0$, $C \sim -1$. As seen from Fig. 4, the general order of accuracy in the different models in representing all three solutions in the region where they exist is GV, GM, IM, and HP with GV most accurate. QG only gives one solution and therefore misses this multiple steady solution aspect of behavior of the SWE altogether. We note that the steady solutions for the intermediate models, obtained from the respective higher order polynomials for T, can include additional roots that satisfy (5.9), but that do not correspond to any solutions of the SWE. These typically involve extreme values of R or Q and are not discussed further here.

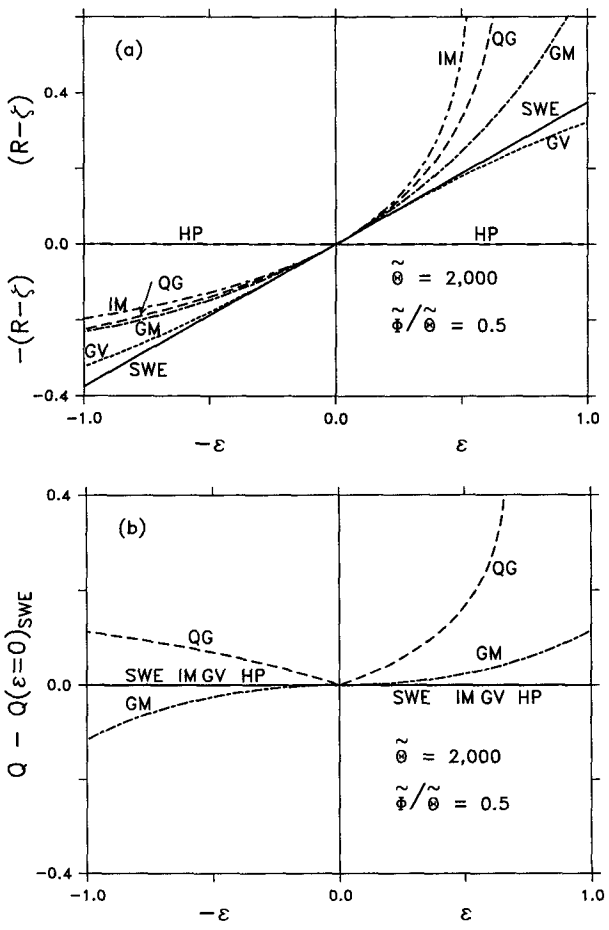

FIG. 3. Exact solutions for the steady flow in an elliptic paraboloid with $\tilde{\theta} = 2000$ and $\tilde{\phi}/\tilde{\theta} = 0.5$. Plots are the same as in Fig. 2.

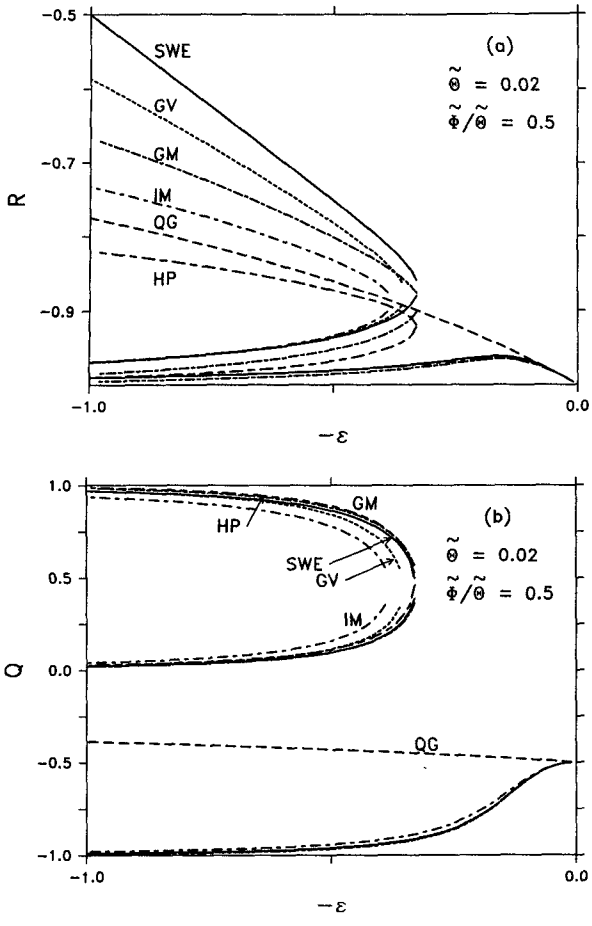

FIG. 4. Exact solutions for the steady flow in an elliptic paraboloid with $\zeta = -1$, $\tilde{\theta} = 0.02$, and $\tilde{\phi}/\tilde{\theta} = 0.5$; (a) R vs $-\epsilon$ for $0 \leq \epsilon < 1$; (b) Q vs $-\epsilon$. For these values of ζ, $\tilde{\theta}$ and $\tilde{\phi}/\tilde{\theta}$, three steady solutions satisfying (5.9) exist for the SWE when $\epsilon > 0.327$.

Next we consider the unsteady flow problem for $0 \leq \epsilon < 1$ with $\zeta = -1$ and with L_0^2 specified so that (5.25) and (5.26) are satisfied. We assume $\zeta = -1$ since the physically realizable solutions primarily occur for negative vorticity. Results for the rotating elliptical eddy (Rodon) solution with no topography ($\tilde{\theta} = 0$) and with $L_0^2 = 0.1$ are shown in Fig. 5. Recall the Rodon solution corresponds to an elliptic vortex of fixed shape that rotates steadily clockwise with angular frequency $\frac{1}{2}|\epsilon\omega|$. The frequency $\epsilon\omega$ is plotted in Fig. 5 along with $(R - \zeta)$ and Q_0 which determine the shape of the eddy. Note that $\epsilon\omega$ is negative and that $\epsilon\omega \sim 0$ for $\epsilon \to 0$. The most accurate approximations for $\epsilon\omega$ over the range of $0 \leq \epsilon < 1$ ($\zeta = -1$) are given by HP and GM, with larger errors for GV and IM. The QG model gives $\epsilon\omega = 0$ and does not properly represent this time-dependent solution. The structure of the eddy as determined by R and Q_0, on the other hand, is given most accurately by GV and least accurately by HP, with GM and IM in between, similar to the results from the steady solutions.

The effect of the bottom topography of the circular paraboloid on these unsteady motions is shown in Fig. 6 where $\tilde{\theta} = 0.2$ and again $L_0^2 = 0.1$. In this case, the frequency $\epsilon\omega$ at $\epsilon = 0$ is nonzero and positive and there

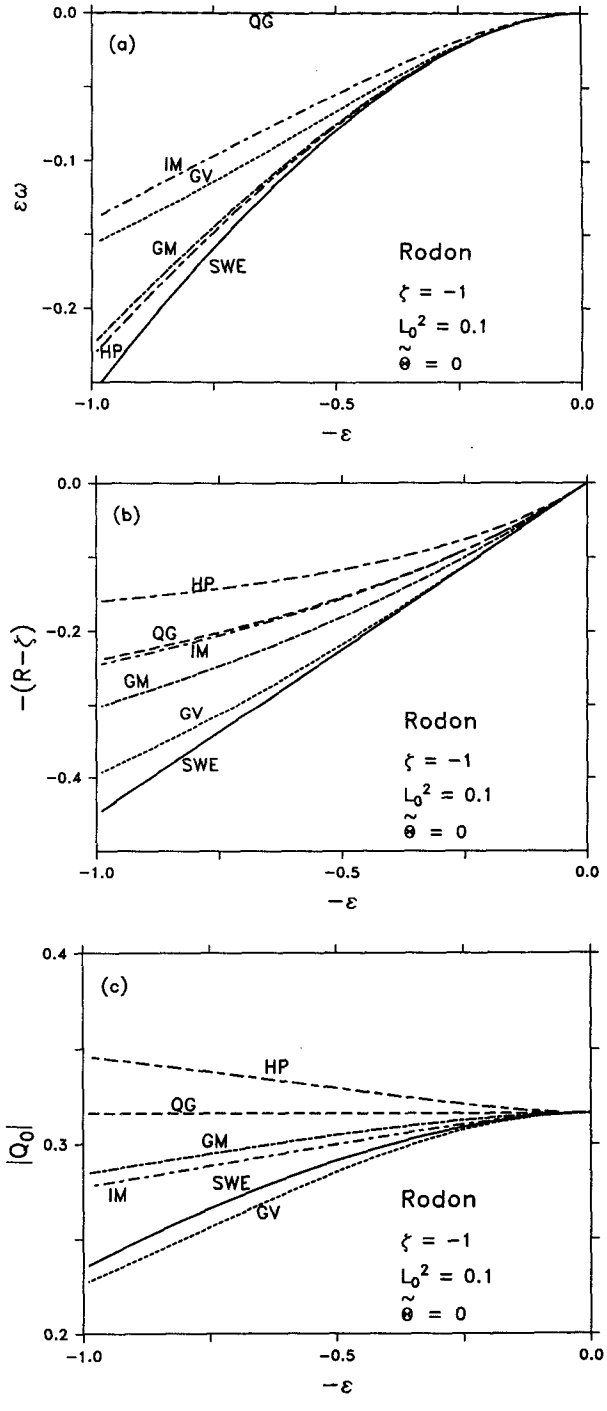

FIG. 5. Exact solutions for the unsteady rotating elliptical eddy (Rodon) with $\zeta = -1$, $L_0^2 = 0.1$, and no topography $\tilde{\theta} = 0$; (a) the frequency $\epsilon\omega$ vs $-\epsilon$ for $0 \leq \epsilon < 1$; (b) $-(R - \zeta)$ vs $-\epsilon$; (c) $|Q_0|$ vs $-\epsilon$.

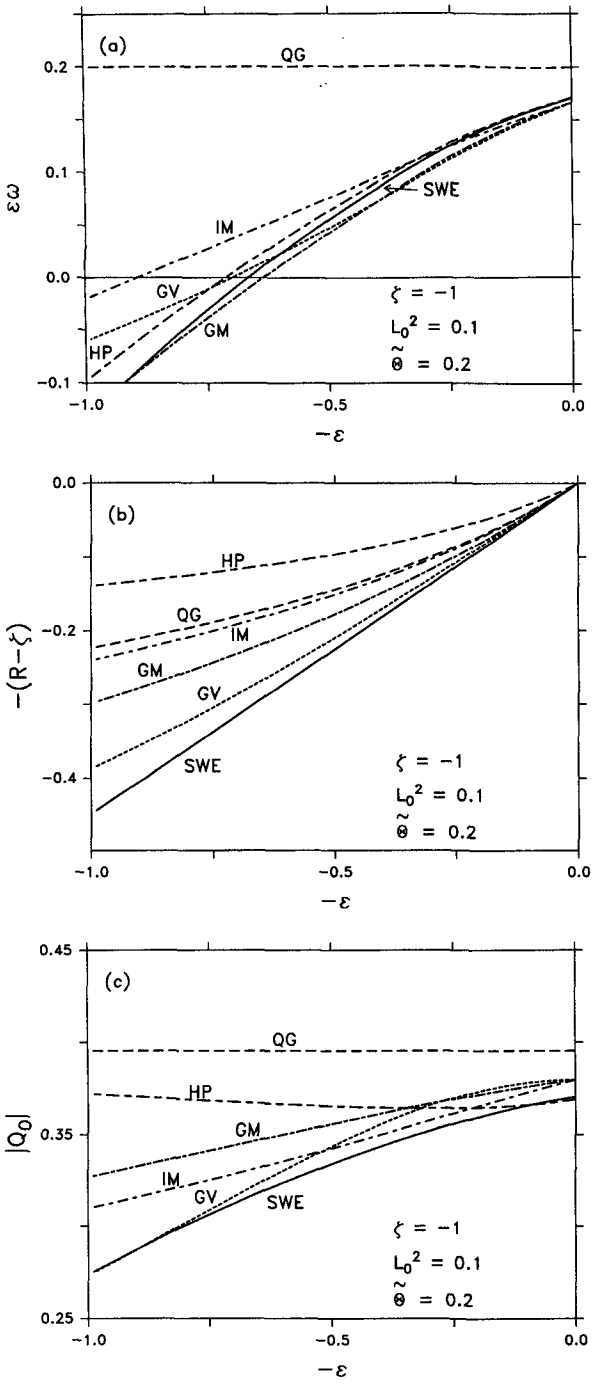

FIG. 6. Exact solutions for the unsteady rotating elliptical eddy in a circular paraboloid with $\zeta = -1$, $L_0^2 = 0.1$ and $\tilde{\theta} = 0.2$; (a) the frequency $\epsilon\omega$ vs $-\epsilon$ for $0 \leq \epsilon < 1$; (b) $-(R - \zeta)$ vs $-\epsilon$; (c) $|Q_0|$ vs $-\epsilon$.

is a small error in $\epsilon\omega$ at $\epsilon = 0$ for most of the intermediate models. When $\epsilon\omega$ is positive, the elliptic vortex rotates counterclockwise. The zero frequency solutions that occur for the SWE and the intermediate models at the intersections of the $\epsilon\omega$ curves with the $\epsilon\omega = 0$ axis correspond to the additional steady solutions in the circular paraboloid with $L^2 \neq 0$ that were mentioned in section 5. In general, HP and GM give the best approximation for $\epsilon\omega$ over the range $0 \leq \epsilon < 1$ with GV retaining accuracy of similar magnitude for $0 \leq \epsilon < 0.6$. IM is noticeably less accurate than the others for $\epsilon > 0.5$. With bottom topography, QG has an oscillatory solution with a nonzero frequency, but unlike the SWE, the resulting $\epsilon\omega$ is a constant and does not vary with ϵ. The accuracy of the representation of the structure of the rotating eddy with topography (Fig. 6b,c) is similar to that found for the Rodon (Fig. 5b). For R, GV is the most accurate, while for Q, IM and GV give the best results overall.

8. Summary of results

Although any conclusions to be drawn from the examination of limiting cases and the comparison of exact solutions have to be qualified by the limited nature of the tests, some general patterns have emerged that are worthy of note.

The intermediate models are capable of representing linear ageostrophic coastally-trapped waves with accuracy that is consistent with the standard linear low-frequency approximations. This is a substantial improvement over the QG approximation where the properties of ageostrophic topographic waves are misrepresented and coastal Kelvin waves are entirely filtered out. On the other hand, the intermediate models reduce to the QG balances in the limit of $\epsilon \to 0$ with small topographic variations $h_B = O(\epsilon)$.

For the particular problems in sections 5 and 6 where exact analytical solutions to both the SWE and the intermediate models can be found and compared, BE, BEM, HBE, NBE, and MSE give the exact solutions of the SWE. This situation unfortunately does not test those particular models as much as we would like and as much as is possible using numerical solutions (see Parts II and III), but the exact solutions available for IM, GV, GM, HP, LBE, LQBE, and QG provide useful comparisons.

The performance of Salmon's (1983) HP model is not as good as some of the other models. The steady circular vortex (Fig. 1) and the time-dependent Rodon (Fig. 5) provide comparisons against SWE solutions in situations that do not involve any bottom topographic variations. Thus, the HP model in those cases is based directly on the equations presented in Salmon (1983). The accuracy of HP for the circular vortex is the poorest of all models and even has larger errors than QG. This is true also for the structure of the elliptical eddy in the Rodon solution, although in that case, HP produces an accurate approximation for the frequency. An additional disconcerting feature of HP that occurs with $h_B = 0$ is the distortion of the dispersion relation for linear coastal Kelvin waves, such that the magnitude of the phase velocity increases as the magnitude of the wavenumber increases (4.20).

When bottom topography ($h_B \neq 0$) is added to HP (appendix A) following the procedure of Salmon (1983), the equations retain conservation laws for geostrophic potential vorticity and geostrophic energy, but the solutions exhibit inaccurate behavior in the limit $F \to 0$. This is most easily demonstrated by the exact solutions for the steady flow in a circular paraboloid. For the SWE and all other approximate models, this solution reduces to that for a circular vortex independent of the paraboloidal shape, but the HP solution (7.2) retains an erroneous dependence on the topography and on F, through the parameter $\tilde{\theta}$. The solutions for the steady flow in an elliptic paraboloid are also misrepresented by HP in the limit $F \to 0$. These results lead us to conclude that, in the presence of bottom topography $h_B \neq 0$, the method of implementation of Salmon's (1983) procedure that is followed in appendix A requires modification. Because this general technique of deriving approximate equations retains conservation laws, it seems to be potentially of great value. The present results indicate, however, that additional work is desirable to determine optimum methods for making approximations in the Lagrangian.

The comparison of the exact solutions shows that in general most of the intermediate models are capable of providing much more accurate solutions than the QG (and LBE, LQBE) approximation. This behavior is particularly clear in the steady case at parameter values for which the SWE and most of the intermediate models possess three possible steady solutions, but QG has only one (Fig. 4). The same point is illustrated for the Rodon solution (Fig. 5) which QG is incapable of representing. For the steady flow and for the structure of the eddy in the unsteady case, the accuracy of the other intermediate models is almost always in the order GV, GM and IM, with GV most accurate and IM occasionally less accurate than QG. It appears from these results that GV and GM both provide substantially better approximations than IM.

Acknowledgments. This research was supported jointly by the National Science Foundation under Grant OCE-8620403, by the Institute for Naval Oceanography under Subcontract No. S8765, and by the Office of Naval Research under Contract N00014-87-K-0009 (Coastal Transition Zone Program). The authors are grateful to R. Salmon, B. Cushman-Roisin, and P. Gent for helpful and insightful discussions. They also thank F. Beyer for typing the manuscript.

APPENDIX A

Salmon's Equations—HP

The method developed by Salmon (1983) to derive approximate equations for nearly geostrophic flow and applied there to the shallow-water equations (without bottom topographic variations) is followed here to obtain approximate equations for the SWE in the case $h_B(x, y) \neq 0$ (see also Miles and Salmon 1985). We use similar notation with the exceptions that here the derivation is with the dimensionless variables defined in section 2 and the Coriolis parameter f is assumed to be a constant.

The positions of marked fluid particles are defined as functions of curvilinear labeling coordinates (a, b) and time τ,

$$x = x(a, b, \tau), \quad y = y(a, b, \tau). \quad \text{(A1a,b)}$$

The labeling coordinates remain constant following fluid particles. The time variable, $\tau = t$, but $\partial/\partial\tau$ means (a, b) are held fixed and

$$\partial/\partial\tau = \partial/\partial t + u\partial/\partial x + v\partial/\partial y. \quad \text{(A2)}$$

The labeling coordinates are defined so that

$$dadb = hdxdy, \quad \text{(A3)}$$

where

$$h = \partial(a, b)/\partial(x, y) = J(a, b). \quad \text{(A4)}$$

The continuity equation (2.3a) follows from the application of $\partial/\partial\tau$ to (A4).

A fluid blob is assumed to be confined to a finite region of space with $h \to 0$ at the fluid boundaries. The shallow-water momentum equations (2.1b, c) and the relations

$$u = \partial x/\partial\tau, \quad v = \partial y/\partial\tau, \quad \text{(A5a,b)}$$

follow from the application of Hamilton's principle in modified form,

$$\delta \int_{-\infty}^{+\infty} L d\tau = 0, \quad \text{(A6)}$$

to the Lagrangian.

$$L = \iint dadb \left\{ \left(\epsilon u - \frac{1}{2} y \right) \frac{\partial x}{\partial \tau} + \left(\epsilon v + \frac{1}{2} x \right) \frac{\partial y}{\partial \tau} - \frac{1}{2} [\epsilon(u^2 + v^2) + (\epsilon F)^{-1}(h + 2h_B)] \right\}, \quad \text{(A7)}$$

where the integrations over a and b extend over the entire fluid blob and where δ stands for arbitrary independent variations δx, δy, δu, $\delta v(a, b, \tau)$ in the fluid particle positions and velocities. The variations vanish as $\tau \to \pm\infty$.

Salmon's (1983) method for deriving approximate equations for nearly geostrophic flow consists of replacing u and v in L by their geostrophic values to form the Lagrangian

$$L_1 = \iint dadb \left\{ \left(\epsilon u_G - \frac{1}{2} y \right) \frac{\partial x}{\partial \tau} + \left(\epsilon v_G + \frac{1}{2} x \right) \frac{\partial y}{\partial \tau} - \frac{1}{2} [\epsilon(u_G^2 + v_G^2) + (\epsilon F)^{-1}(h + 2h_B)] \right\}, \quad \text{(A8)}$$

where

$$u_G = -\eta_y = -(h_y + h_{By})/\epsilon F, \quad \text{(A9a)}$$

$$v_G = \eta_x = (h_x + h_{Bx})/\epsilon F, \quad \text{(A9b)}$$

The application of Hamilton's Principle to L_1,

$$\delta \int_{-\infty}^{+\infty} L_1 d\tau = 0, \quad \text{(A10)}$$

where independent variations are taken in particle locations, δx, δy, and where

$$\delta\eta = (\delta h + h_{Bx}\delta x + h_{By}\delta y)/\epsilon F, \quad \text{(A11)}$$

results in the approximate momentum equations (3.23) where

$$\epsilon u_A = \partial x/\partial\tau - u_G, \quad \epsilon v_A = \partial y/\partial\tau - v_G. \quad \text{(A12a,b)}$$

Since the approximation L_1 retains the symmetry properties of L concerning invariance to particle relabeling and to translations in time, the approximate dynamics (A10) possesses conservation laws for geostrophic potential vorticity (3.12) on fluid particles and for geostrophic energy [(A18) below].

The following diagnostic equations for u_A and v_A insure consistency between (2.1a) and (3.23) and are derived by combining the x or y derivative of (2.1a) with (3.23a) or (3.23b) to eliminate the time derivative η_{xt} or η_{yt}:

$$\nabla^2(hu_A) - F(1 + \epsilon\nabla^2\eta)u_A = F(u_G v_{Gx} + v_G v_{Gy}) + \epsilon^{-1}N_x, \quad \text{(A13a)}$$

$$\nabla^2(hv_A) - F(1 + \epsilon\nabla^2\eta)v_A = -F(u_G u_{Gx} + v_G u_{Gy}) + \epsilon^{-1}N_y, \quad \text{(A13b)}$$

where

$$N = (u_G h_{Bx} + v_G h_{By}). \quad \text{(A13c)}$$

Note that (A13a, b) are uncoupled linear equations for u_A and v_A assuming η is known. Since $h > 0$, the condition $(1 + \epsilon\nabla^2\eta) > 0$ insures that the coefficient of u_A or v_A on the left hand side of (A13a, b) is of opposite sign to that of the highest derivative terms $h\nabla^2 u_A$ or $h\nabla^2 v_A$. Thus, with appropriate boundary conditions for u_A and v_A, discussed below, unique solutions exist provided $(1 + \epsilon\nabla^2\eta) > 0$ (Garabedian 1964, Chaps. 7, 8).

The equation expressing conservation of geostrophic energy may be derived by multiplying (3.23a) by hu_G, (3.23b) by hv_G, (2.1a) by K_G, (2.1a) by h, combining and using (A13a, b) to obtain

$$\epsilon(hK_G + \tfrac{1}{2}F\eta^2)_t + (hu\mathcal{B}_G)_x + (hv\mathcal{B}_G)_y + \epsilon[hu_G G + h^2 u_G\zeta_A + hv_A N + \epsilon(u_A h^2 v_{Ax} - v_A h^2 u_{Ax})]_x + \epsilon[hv_G G + h^2 v_G\zeta_A - hu_A N + \epsilon(u_A h^2 v_{Ay} - v_A h^2 u_{Ay})]_y = 0, \quad \text{(A14a)}$$

where K_G and $\mathcal{B}_B$ are defined in (3.4d, e) and

$$G = -u_A h_y + v_A h_x. \quad \text{(A14b)}$$

To examine energy conservation in finite regions bounded by solid walls, we integrate (A14) over an area, assumed for convenience to be rectangular, $x_1 \leq x \leq x_2$, $y_1 \leq y \leq y_2$, with no-normal flow conditions of

$$v = v_G + \epsilon v_A = 0, \quad \text{at} \quad y = y_1, y_2, \quad \text{(A15a)}$$

$$u = u_G + \epsilon u_A = 0, \quad \text{at} \quad x = x_1, x_2, \quad \text{(A15b)}$$

to obtain

$$\left[\int_{x_1}^{x_2}\int_{y_1}^{y_2} dxdy\left(hK_G + \tfrac{1}{2}F\eta^2\right)\right]_t + \int_{y_1}^{y_2} dy \times \left[\tfrac{1}{2}(h^2u_A^2)_y + hv_A(u_G v_G - hu_{Ax} + v_G h_{By})\right]\Big|_{x_1}^{x_2} + \int_{x_1}^{x_2} dx\left[-\tfrac{1}{2}(h^2v_A^2)_x + hu_A(u_G v_G + hv_{Ay} - u_G h_{Bx})\right]\Big|_{y_1}^{y_2} = 0. \quad \text{(A16)}$$

We expect the contributions in (A16) from the boundary terms to vanish. This will occur if

$$u_A = 0, \quad \text{at} \quad y = y_1, y_2, \quad \text{(A17a)}$$

$$v_A = 0, \quad \text{at} \quad x = x_1, x_2, \quad \text{(A17b)}$$

in which case (A16) reduces to

$$\left[\int_{x_1}^{x_2}\int_{y_1}^{y_2} dxdy\left(hK_G + \tfrac{1}{2}F\eta^2\right)\right]_t = 0, \quad \text{(A18)}$$

expressing the conservation of geostrophic energy.

The conditions (A17a,b) are consistent with results from the full shallow-water equations (2.1) for which the no-normal-flow conditions (A15) imply

$$u = -\eta_y = u_G, \quad \text{at} \quad y = y_1, y_2, \quad \text{(A19a)}$$

$$v = \eta_x = v_G, \quad \text{at} \quad x = x_1, x_2. \quad \text{(A19b)}$$

Note in addition that (A13a, b) require boundary conditions on u_A and v_A on all boundaries, whereas (A15a, b) only provide conditions on the normal component. Consequently, since (A17a, b) provide needed boundary conditions, since they are consistent with the shallow-water equations, and since they insure the conservation of energy in bounded regions, we infer that they are proper additional boundary conditions for (2.1a), (3.23a, b), and (A13a, b).

For use in section 4b, we record the linear limit of (A13a, b):

$$\nabla^2(Hu_A) - Fu_A = \epsilon^{-1}N_x, \quad \text{(A20a)}$$

$$\nabla^2(Hv_A) - Fv_A = \epsilon^{-1}N_y. \quad \text{(A20b)}$$

APPENDIX B

Solution Procedures for NBE, HBE, BE, and BEM

In Part II, numerical finite difference solutions in doubly periodic domains are obtained for NBE by solving the two coupled governing equations for ψ_0 and η (3.49) and (3.52). The balance equation (3.49), when regarded as a single equation for ψ_0 with η known, is a nonlinear Monge-Ampére equation (Charney 1955; Bolin 1955) which may be either elliptic [when $(1 + 2\epsilon\nabla^2\eta) > 0$] or hyperbolic. For the coupled nonlinear system (3.49) and (3.52), the requirements for a well-posed mathematical problem are not obvious (see the discussion for BE in Gent and McWilliams 1983a). We outline below the method used to obtain numerical solutions for NBE in Part II. This involves effectively solving (3.49) for η with ψ_0 regarded as known. A similar procedure has also been applied to (3.42) and (3.43) for HBE.

We drop the subscript on ψ_0 and let

$$\eta = \psi + \epsilon\eta', \tag{B1}$$

so that (3.52) and (3.49) may be written

$$(h_R\psi_{xt})_x + (h_R\psi_{yt})_y - F\psi_t = \epsilon F\eta'_t - \epsilon^{-1}J(h_R, \mathcal{B}_R), \tag{B2}$$

and

$$\nabla^2\eta' = 2J(\psi_x, \psi_y). \tag{B3}$$

To solve (B2) and (B3) and to step forward in time an iteration procedure is utilized. With both ψ and η' assumed to be known at a given time $t = t_n$ (designated by ψ^n, η'^n) and at previous times, an estimate for $\eta_t'^n$ is obtained from simple extrapolation of η'^n in time. This estimate is substituted in (B2), which is then solved as a linear equation in ψ_t^n. The condition $(1 + \epsilon\nabla^2\psi) > 0$ implies $h_R > 0$ and insures the retention of opposite signs for $h_R\nabla^2\psi_t$ and $F\psi_t$. An estimate of ψ^{n+1} at the new time $t = t_{n+1}$ is obtained from ψ_t^n and substituted in the right hand side of (B3), which is then solved as a linear Poisson equation for η'^{n+1}. This gives a new estimate for $\eta_t'^n$ in (B2) and the cycle is repeated until convergence for ψ^{n+1} and η'^{n+1} is obtained.

For BE, numerical solutions are obtained in Part II using the technique of Norton et al. (1986). We present here another method that we utilize for the solution of BEM in Part II and for BE and BEM in the channel flows in Part III. In addition, this procedure is based on a formulation that may be utilized for most of the other models (see appendix C). The solution procedure has some points in common with that outlined above for NBE and is essentially an extension of that utilized for QG when χ is also determined. In the latter case, η_{0t} is found from the solution of (2.23) and χ is subsequently obtained from the solution of $\nabla^2\chi = D_1$, where D_1 is given by either (2.17) or (2.19). For BE, we represent η as in (B1) and utilize (2.9), (3.29) and (3.30), which may be written

$$(\nabla^2\psi - F\psi)_t = \epsilon F\eta'_t - J(\psi, \zeta - \tilde{H}) - \epsilon[\chi_x(\zeta - \tilde{H})]_x - \epsilon[\chi_y(\zeta - \tilde{H})]_y, \tag{B4a}$$

$$\nabla^2\eta' = 2J(\psi_x, \psi_y), \tag{B4b}$$

$$\nabla^2\chi = -J(\psi, \zeta) - \epsilon(\chi_x\zeta)_x - \epsilon(\chi_y\zeta)_y - \zeta_t. \tag{B4c}$$

Iteration is utilized to solve (B4a, b, c). Two different methods may be employed. These are briefly outlined here. More details are given in Parts II and III. In the first method, ψ^n, η'^n, χ^{n-1}, ψ_t^{n-1}, and $\eta_t'^{n-1}$ are assumed to be known and (B4a, b, c) are solved iteratively for ψ_t^n, $\eta_t'^n$ (and hence ψ^{n+1}, η'^{n+1}), and χ^n. The procedure starts by simple extrapolation in time to find estimates for $\eta_t'^n$ and χ^n. These are used in (B4a) which is solved for ψ_t^n. This gives values for ψ^{n+1} and ζ_t^n for use in (B4b) and (B4c) which are solved for new estimates of η'^{n+1} (and hence $\eta_t'^n$) and χ^n, respectively. The process is repeated until it converges.

The second method of solution is based on the iteration scheme developed for application to (3.29), (3.30) and (3.31) by Norton et al. (1986). In this case, ψ^n, η'^n, χ^n, ψ_t^n, and $\eta_t'^n$ are assumed to be known and iteration of (B4a, b, c) is used to provide new values for all of these variables at t_{n+1}. This method is utilized in Parts II and III to obtain solutions for BEM, since (3.45) required that χ be found simultaneously with ψ and η' at the same time level. In addition, a solution procedure based on (3.29), (3.45), and a modified omega equation (3.31) is not as appropriate for BEM because the form of (3.45) results in the presence of χ_t in an omega equation.

APPENDIX C

Intermediate Model Summary

The differences in the approximations involved in the various intermediate models can be most readily appreciated if the models are formulated in a common manner. It is possible to do this based on the representation of BE discussed in section 3e and appendix B. The governing equations in this form for the intermediate models described in section 3, for QG, and for SWE, are summarized below (SE is omitted). As in (3.26), the velocity components are represented by

$$u = -\psi_y + \epsilon\chi_x, \quad v = \psi_x + \epsilon\chi_y, \tag{C1a,b}$$

and recall from (2.10) and (3.4c) that

$$\tilde{H} = \hat{H}/\epsilon = F\eta - \epsilon^{-1}h_B, \quad \zeta_G = \nabla^2\eta. \tag{C2a,b}$$

BE:

$$(\nabla^2\psi - F\eta)_t = -J(\psi, \zeta - \tilde{H}) - \epsilon[\chi_x(\zeta - \tilde{H})]_x - \epsilon[\chi_y(\zeta - \tilde{H})]_y, \tag{C3a}$$

$$\zeta = \nabla^2\psi = \nabla^2\eta - \epsilon 2J(\psi_x, \psi_y), \quad \text{(C3b)}$$

$$\nabla^2\chi = -J(\psi, \zeta) - \epsilon(\chi_x\zeta)_x - \epsilon(\chi_y\zeta)_y - \zeta_t. \quad \text{(C3c)}$$

QG:

$$(\nabla^2\eta - F\eta)_t = -J(\eta, \zeta_G - \tilde{H}), \quad \text{(C4a)}$$

$$\nabla^2\chi = -J(\eta, \zeta_G) - \zeta_{Gt}. \quad \text{(C4b)}$$

LBE:

$$(\nabla^2\eta - F\eta)_t = -J(\eta, \zeta_G - \tilde{H}) + \epsilon(\chi_x\tilde{H})_x + \epsilon(\chi_y\tilde{H})_y, \quad \text{(C5a)}$$

$$\nabla^2\chi = -J(\eta, \zeta_G) - \zeta_{Gt}. \quad \text{(C5b)}$$

LQBE:

$$(\nabla^2\eta - F\eta)_t = -J(\eta, \zeta_G - \tilde{H}) - \epsilon[\chi_x(\zeta_G - \tilde{H})]_x - \epsilon[\chi_y(\zeta_G - \tilde{H})]_y, \quad \text{(C6a)}$$

$$\nabla^2\chi = -J(\eta, \zeta_G) - \epsilon(\chi_x\zeta_G)_x - \epsilon(\chi_y\zeta_G)_y - \zeta_{Gt}. \quad \text{(C6b)}$$

HBE:

$$(\nabla^2\psi - F\eta)_t = -J(\psi, \zeta - \tilde{H}) + \epsilon(\chi_x\tilde{H})_x + \epsilon(\chi_y\tilde{H})_y, \quad \text{(C7a)}$$

$$\zeta = \nabla^2\psi = \nabla^2\eta - \epsilon 2J(\psi_x, \psi_y), \quad \text{(C7b)}$$

$$\nabla^2\chi = -J(\psi, \zeta) - \zeta_t. \quad \text{(C7c)}$$

BEM:

$$(\nabla^2\psi - F\eta)_t = -J(\psi, \zeta - \tilde{H}) - \epsilon[\chi_x(\zeta - \tilde{H})]_x - \epsilon[\chi_y(\zeta - \tilde{H})]_y, \quad \text{(C8a)}$$

$$\zeta = \nabla^2\psi = \nabla^2\eta - \epsilon 2J(\psi_x, \psi_y) - \epsilon^2 J(\zeta, \chi), \quad \text{(C8b)}$$

$$\nabla^2\chi = -J(\psi, \zeta) - \epsilon(\chi_x\zeta)_x - \epsilon(\chi_y\zeta)_y - \zeta_t. \quad \text{(C8c)}$$

NBE:

$$\psi = \psi_0 + \epsilon^2\psi_1, \quad \text{(C9a)}$$

$$(\nabla^2\psi_0 - F\eta)_t = -J(\psi, \zeta_0 - \tilde{H}) - \epsilon[\chi_x(\zeta_0 - \tilde{H})]_x - \epsilon[\chi_y(\zeta_0 - \tilde{H})]_y, \quad \text{(C9b)}$$

$$\zeta_0 = \nabla^2\psi_0 = \nabla^2\eta - \epsilon 2J(\psi_{0x}, \psi_{0y}), \quad \text{(C9c)}$$

$$\zeta_1 = \nabla^2\psi_1 = -J(\zeta_0, \chi) - \epsilon(\psi_{1x}\zeta_0)_x - \epsilon(\psi_{1y}\zeta_0)_y, \quad \text{(C9d)}$$

$$\nabla^2\chi = -J(\psi, \zeta_0) - \epsilon(\chi_x\zeta_0)_x - \epsilon(\chi_y\zeta_0)_y - \zeta_{0t}. \quad \text{(C9e)}$$

IM:

$$(\nabla^2\eta - F\eta)_t = -J(\eta, \zeta_G) + J(\psi, \tilde{H}) + \epsilon(\chi_x\tilde{H})_x + \epsilon(\chi_y\tilde{H})_y, \quad \text{(C10a)}$$

$$\zeta = \nabla^2\psi = \nabla^2\eta - \epsilon 2J(\eta_x, \eta_y), \quad \text{(C10b)}$$

$$\nabla^2\chi = -J(\eta, \zeta_G) - \zeta_{Gt}. \quad \text{(C10c)}$$

GV:

$$(\nabla^2\eta - F\eta)_t = -J(\psi, \zeta_G - \tilde{H}) - \epsilon[\chi_x(\zeta_G - \tilde{H})]_x - \epsilon[\chi_y(\zeta_G - \tilde{H})]_y, \quad \text{(C11a)}$$

$$\zeta = \nabla^2\psi = \nabla^2\eta + \epsilon\nabla^2 K_G - \epsilon(\psi_x\zeta_G)_x - \epsilon(\psi_y\zeta_G)_y - \epsilon^2 J(\zeta_G, \chi), \quad \text{(C11b)}$$

$$\nabla^2\chi = -J(\psi, \zeta_G) - \epsilon(\chi_x\zeta_G)_x - \epsilon(\chi_y\zeta_G)_y - \zeta_{Gt}. \quad \text{(C11c)}$$

GM:

$$(\zeta_{GM} - F\eta)_t = -J(\psi, \zeta_{GM} - \tilde{H}) - \epsilon[\chi_x(\zeta_{GM} - \tilde{H})]_x - \epsilon[\chi_y(\zeta_{GM} - \tilde{H})]_y, \quad \text{(C12a)}$$

$$\zeta = \nabla^2\psi = \nabla^2\eta - \epsilon[J(\eta_x, \psi_y) + J(\psi_x, \eta_y)] + \epsilon^2[J(\eta_x, \chi_x) + J(\eta_y, \chi_y)], \quad \text{(C12b)}$$

$$\nabla^2\chi = -J(\psi, \zeta_{GM}) - \epsilon(\chi_x\zeta_{GM})_x - \epsilon(\chi_y\zeta_{GM})_y - \zeta_{GMt}, \quad \text{(C12c)}$$

$$\zeta_{GM} = \nabla^2\eta + \epsilon J(\eta_x, \eta_y). \quad \text{(C12d)}$$

HP:

$$(\nabla^2\eta - F\eta)_t = -J(\psi, \zeta_G - \tilde{H}) - \epsilon[\chi_x(\zeta_G - \tilde{H})]_x - \epsilon[\chi_y(\zeta_G - \tilde{H})]_y, \quad \text{(C13a)}$$

$$\zeta = \nabla^2\psi = \nabla^2\eta + \nabla^2\hat{\mathcal{B}}_{HP} - \epsilon(\psi_x\zeta_G)_x - \epsilon(\psi_y\zeta_G)_y - \epsilon^2 J(\zeta_G, \chi), \quad \text{(C13b)}$$

$$\nabla^2\chi = -J(\psi, \zeta_G) - \epsilon(\chi_x\zeta_G)_x - \epsilon(\chi_y\zeta_G)_y - \zeta_{Gt}, \quad \text{(C13c)}$$

$$\hat{\mathcal{B}}_{HP} = \mathcal{B}_{HP} - \eta = \epsilon[\psi_y\eta_y + \psi_x\eta_x - K_G + \epsilon J(\eta, \chi)] + F^{-1}h(\zeta - \zeta_G) - F^{-1}[(\psi_y - \eta_y)h_{By} + (\psi_x - \eta_x)h_{Bx} + \epsilon J(h_B, \chi)]. \quad \text{(C13d)}$$

MSE:

$$(\nabla^2\psi - F\eta)_t = -J(\psi, \zeta - \tilde{H}) - \epsilon[\chi_x(\zeta - \tilde{H})]_x - \epsilon[\chi_y(\zeta - \tilde{H})]_y, \quad \text{(C14a)}$$

$$\zeta = \nabla^2\psi = \nabla^2\eta - \epsilon 2J(\psi_x, \psi_y) - \epsilon^2 Z, \quad \text{(C14b)}$$

$$Z = 2[J(\chi_x, \psi_x) + J(\chi_y, \psi_y) + \epsilon J(\chi_x, \chi_y)] - J(\psi, \nabla^2\chi) - \epsilon(\chi_x\nabla^2\chi)_x - \epsilon(\chi_y\nabla^2\chi)_y, \quad \text{(C14c)}$$

$$\nabla^2\chi = -\epsilon^{-1}D' - J(\psi, \zeta) - \epsilon(\chi_x\zeta)_x - \epsilon(\chi_y\zeta)_y - \zeta_t, \quad \text{(C14d)}$$

$$\nabla^2 D' - FD' = \epsilon^2 F[2J(\psi_x, \psi_y) + \epsilon Z]_t. \quad \text{(C14e)}$$

SWE:

$$(\nabla^2\psi - F\eta)_t = -J(\psi, \zeta - \tilde{H}) - \epsilon[\chi_x(\zeta - \tilde{H})]_x - \epsilon[\chi_y(\zeta - \tilde{H})]_y, \quad \text{(C15a)}$$

$$\zeta = \nabla^2\psi = \nabla^2\eta - \epsilon 2J(\psi_x, \psi_y) - \epsilon^2 Z + \epsilon^2\nabla^2\chi_t, \quad \text{(C15b)}$$

$$\nabla^2\chi = -J(\psi, \zeta) - \epsilon(\chi_x\zeta)_x - \epsilon(\chi_y\zeta)_y - \zeta_t. \quad \text{(C15c)}$$

The formulation (C14) for MSE is not the most natural one because it results in the appearance of Z_t, and hence χ_t, in (C14e) which makes it awkward for use in obtaining numerical solutions. The alternative employment of (3.56) to find $D = \epsilon\nabla^2\chi$ (and hence χ) in place of (C14d, e), as is done in Part II, avoids this difficulty. Note that this is opposite to the situation with BEM, as mentioned in appendix B, where χ_t appears in an omega equation, but not in (C8a, b, c).

If we consider QG derived from (3.4a, b) and (3.8), LBE from (3.4a, b) and (3.35), and LQBE from (3.38a, b) and (3.35), as discussed in sections 3a, 3f, and 3g, the approximate balance equation (C10b) from IM also applies to QG and LBE, while

$$\zeta = \nabla^2\psi = \nabla^2\eta - \epsilon 2J(\eta_x, \eta_y) - \epsilon^2 J(\zeta_G, \chi), \quad \text{(C16)}$$

holds for LQBE.

REFERENCES

Allen, J. S., and P. K. Kundu, 1978: On the momentum, vorticity, and mass balance on the Oregon shelf. *J. Phys. Oceanogr.*, **8**, 13–27.

——, J. A. Barth and P. A. Newberger, 1990: On intermediate models for barotropic continental shelf and slope flow fields: Part III, comparison of numerical model solutions in periodic channels. *J. Phys. Oceanogr.*, submitted.

Ball, F. K., 1965: The effect of rotation on the simpler modes of motion of a liquid in an elliptic paraboloid. *J. Fluid Mech.*, **22**, 529–545.

Barth, J. A., J. S. Allen and P. A. Newberger, 1990: On intermediate models for barotropic continental shelf and slope flow fields: Part II, comparison of numerical model solutions in doubly-periodic domains. *J. Phys. Oceanogr.*, **20**, 1044–1076.

Bolin, B., 1955: Numerical forecasting with the barotropic model. *Tellus*, **7**, 27–49.

——, 1956: An improved barotropic model and some aspects of using the balance equations for three-dimensional flow. *Tellus*, **8**, 61–75.

Charney, J. G., 1955: The use of primitive equations of motion in numerical prediction. *Tellus*, **7**, 22–26.

——, 1962: Integration of the primitive and the balance equations, *Proc. Int. Symp. Numerical Weather Prediction*, Tokyo, Meteor. Soc. Japan, 131–152.

Cushman-Roisin, B., 1986: Frontal geostrophic dynamics. *J. Phys. Oceanogr.*, **16**, 132–143.

——, 1987: Exact analytical solutions for elliptical vortices of the shallow-water equations. *Tellus*, **39A**, 235–244.

——, W. H. Heil and D. Nof, 1985: Oscillations and rotations of elliptic warm-core rings. *J. Geophys. Res.*, **40**, 11 756–11 764.

Denbo, D. W., and J. S. Allen, 1987: Large scale response to atmospheric forcing of shelf currents and coastal sea level off the west coast of North America: May–July, 1981 and 1982. *J. Geophys. Res.*, **92**, 1757–1782.

Eliassen, A., 1948: The quasi-static equations of motion with pressure as independent variable. *Geofys. Publ.*, **17**, No. 3.

Garabedian, P. R., 1964: *Partial Differential Equations*. John Wiley & Sons, Inc., New York, 672 pp.

Gent, P. R., and J. C. McWilliams, 1982: Intermediate model solutions to the Lorenz equations: strange attractors and other phenomena. *J. Atmos. Sci.*, **39**, 3–13.

——, and J. C. McWilliams, 1983a: Consistent balanced models in bounded and periodic domains. *Dyn. Atmos. Oceans*, **7**, 67–93.

——, and J. C. McWilliams, 1983b: Regimes of validity for balanced models. *Dyn. Atmos. Oceans*, **7**, 167–183.

——, and J. C. McWilliams, 1984: Balanced models in isentropic coordinates and the shallow-water equations. *Tellus*, **36A**, 166–171.

Hoskins, B. J., 1975: The geostrophic momentum approximation and the semigeostrophic equations. *J. Atmos. Sci.*, **32**, 233–242.

——, 1982: The mathematical theory of frontogenesis. *Ann. Rev. Fluid Mech.*, **14**, 131–151.

Hukuda, H. and T. Yamagata, 1988: A unified geostrophic equation with application to a cold core ring. *Tellus*, **40A**, 407–418.

Huyer, A., and P. M. Kosro, 1987: Mesoscale surveys over the shelf and slope in the upwelling region near Point Arena, California. *J. Geophys. Res.*, **92**, 1655–1681.

Kosro, P., and A. Huyer, 1986: CTD and velocity surveys of seaward jets off northern California, July 1981 and 1982. *J. Geophys. Res.*, **91**, 7680–7690.

Lorenz, E. N., 1960: Energy and numerical weather prediction. *Tellus*, **12**, 364–373.

Lynch, P., 1989: The slow equations. *Q. J. R. Meteorol. Soc.*, **115**, 201–219.

McWilliams, J. C., 1977: A note on a consistent quasi-geostrophic model in a multiply connected domain. *Dyn. Atmos. Oceans*, **1**, 427–441.

——, and P. R. Gent, 1980: Intermediate models of planetary circulations in the atmosphere and ocean. *J. Atmos. Sci.*, **37**, 1657–1678.

——, P. R. Gent and N. J. Norton, 1986: The evolution of balanced, low-mode vortices on the β-plane. *J. Phys. Oceanogr.*, **16**, 838–855.

Miles, J., and R. Salmon, 1985: Weakly dispersive nonlinear gravity waves. *J. Fluid Mech.*, **157**, 519–531.

Norton, N. J., J. C. McWilliams and P. R. Gent, 1986: A numerical model of the balance equations in a periodic domain and an example of balanced turbulence. *J. Comput. Phys.*, **67**, 439–471.

Pedlosky, J., 1987: *Geophysical Fluid Dynamics*, Springer-Verlag, New York, 710 pp.

Robinson, A. R., J. A. Carton, C. N. K. Mooers, L. J. Walstad, E. F. Carter, M. M. Rienecker, J. A. Smith and W. G. Leslie, 1984: A real-time dynamical forecast of ocean synoptic/mesoscale eddies. *Nature*, **309**, 781–783.

——, J. A. Carton, J. Pinardi and C. N. K. Mooers, 1986: Dynamical forecasting and dynamical interpolation: an experiment in the California Current. *J. Phys. Oceanogr.*, **16**, 1561–1579.

Salmon, R., 1983: Practical use of Hamilton's principle. *J. Fluid Mech.*, **132**, 431–444.

——, 1985: New equations for nearly geostrophic flow. *J. Fluid Mech.*, **153**, 461–477.

——, 1988a: Hamiltonian Fluid Mechanics. *Ann. Rev. Fluid Mech.*, **20**, 225–256.

——, 1988b: Semigeostrophic theory as a Dirac-bracket projection. *J. Fluid Mech.*, **196**, 345–358.

Schär, C., and H. C. Davies, 1988: Quasi-geostrophic stratified flow over isolated finite amplitude topography. *Dyn. Atmos. Oceans*, **11**, 287–306.

Sutyrin, G. G., and I. G. Yushina, 1986a: Interaction of synoptic eddies of finite amplitude. *Dokl. Akad. Nauk. SSSR*, **288**, 585–589.

——, and ——, 1986b: On the evolution of isolated eddies in a rotating fluid. *Izv. Acad. Nauk. SSSR, Mekh. Zhidk. Gaza*, **4**, 52–59.

——, and ——, 1988: Formation of a vortex soliton. *Dokl. Akad. Nauk. SSSR*, **299**, 580–584.

Williams, G. P., 1985: Geostrophic regimes on a sphere and a beta plane. *J. Atmos. Sci.*, **42**, 1237–1243.

Young, W. R., 1986: Elliptic vortices in shallow water. *J. Fluid Mech.*, **171**, 101–119.